Master's thesis
Master's Programme in Atmospheric Sciences
Aerosol Physics

Studying the effective condensation sink based on heterogeneous nucleation theory and measurements in Beijing

Saana Tuovinen

September 11, 2019

Supervisor(s): Markku Kulmala, Jenni Kontkanen

Examiner(s): Tuukka Petäjä, Veli-Matti Kerminen

University of Helsinki
Faculty of Science

PL 64 (Gustaf Hällströmin katu 2a)
00014 University of Helsinki

HELSINGIN YLIOPISTO — HELSINGFORS UNIVERSITET — UNIVERSITY OF HELSINKI

Tiedekunta — Fakultet — Faculty	Koulutusohjelma — Utbildningsprogram — Degree programme
Faculty of Science	Master's Programme in Atmospheric Sciences Aerosol Physics

Tekijä — Författare — Author

Saana Tuovinen

Työn nimi — Arbetets titel — Title

Studying the effective condensation sink based on heterogeneous nucleation theory and measurements in Beijing

Työn laji — Arbetets art — Level	Aika — Datum — Month and year	Sivumäärä — Sidantal — Number of pages
Master's thesis	September 11, 2019	60

Tiivistelmä — Referat — Abstract

Observations of frequent new particle formation events have been made in severely polluted environments in China. In theory this should not be possible because of the large condensation sink caused by large concentrations of particles. This thesis tries to shed light on reasons why this happens by investigating heterogeneous nucleation in different conditions, for different vapours and seed particles. Especially of interest are those situations where heterogeneous nucleation is considered to be ineffective which would affect the condensation sink of vapours.

Theoretical modelling was used to investigate heterogeneous nucleation and measured data was analyzed to complement theoretical results. In this thesis, special focus is on contact angle θ of heterogeneous nucleation, a variable that depends on surface tensions of the vapour and the seed particle the vapour condenses on. θ has a strong effect on the heterogeneous nucleation probability and the larger it is the less likely nucleation is to occur. Many situations where there was at least in theory little heterogeneous nucleation were found.

Conditions similar to real atmospheric conditions were investigated and contact angles needed for heterogeneous nucleation to be ineffective for a vapour were determined. Because θ is related to chemical properties of the seed particle, aerosol chemical composition was also investigated alongside with the corresponding condensation sink and particle formation rates using data measured in Beijing, China. This was done in hopes of finding indications of if and how effective condensation sink and aerosol chemical composition are related. However, no clear connection was yet found.

Influence of ineffective heterogeneous nucleation on effective condensation sink was considered. It was found that if ineffectiveness of heterogeneous nucleation affects the condensation sink, effective sink can in theory be significantly smaller than condensation sink. Thus, ineffective heterogeneous nucleation due to multiple factors explored in this thesis could in part explain why new particle formation events are observed even in heavily polluted areas.

Avainsanat — Nyckelord — Keywords

Aerosol, Heterogeneous Nucleation, Nucleation, Condensation sink, Effective condensation sink

Säilytyspaikka — Förvaringsställe — Where deposited

Muita tietoja — Övriga uppgifter — Additional information

HELSINGIN YLIOPISTO — HELSINGFORS UNIVERSITET — UNIVERSITY OF HELSINKI

Tiedekunta — Fakultet — Faculty	Koulutusohjelma — Utbildningsprogram — Degree programme
Matemaattis-luonnontieteellinen Tiedekunta	Ilmakehätieteiden maisteriohjelma Aerosolifysiikka

Tekijä — Författare — Author

Saana Tuovinen

Työn nimi — Arbetets titel — Title

Effektiivisen kondensaatiohäviön tutkiminen heterogeeniseen nukleaatioteoriaan ja Pekingissä suoritettujen mittausten pohjalta

Työn laji — Arbetets art — Level	Aika — Datum — Month and year	Sivumäärä — Sidantal — Number of pages
Pro Gradu	23.07.2019	60

Tiivistelmä — Referat — Abstract

Lukuisia hiukkasmuodostumistapahtumia on havaittu hyvin saastuneissa ympäristöissä Kiinassa. Saastuneessa ympäristössä höyryjen kondensaatiohäviö on hyvin suuri, eikä pitäisi teoriassa olla mahdollista, että näitä hiukkasmuodostumistapahtumia havaitaan. Tämä opinnäytetyö pyrkii osaltaan selittämään näitä havaintoja tutkimalla heterogeenista nukleaatiota erilaisissa olosuhteissa, erilaisille kondensoituville höyryille ja erilaisille hiukkasytimille. Pyrkimyksenä on löytää tilanteita, joissa heterogeenista nukleaatiota ei tapahdu tietyille höyryille ja tutkia kuinka tämä vaikuttaa kondensaatiohäviöön.

Heterogeenista nukleaatiota tutkittiin teoreettisesti mallintaen. Tässä työssä tarkastellaan erityisesti heterogeenisen nukleaation kontaktikulmaa θ. θ riippuu höyryn ja ytimen pintajännityksistä ja sillä on vahva vaikutus heterogeenisen nukleaation todennäköisyyteen. Suuremmilla kontaktikulmilla heterogeeninen nukleaatiotodennäköisyys on pienempi. Monia sellaisia tilanteita, joissa ei ainakaan teoriassa ole heterogeenista nukleaatiota, löydettiin. Tällaisia tilanteita voi syntyä esimerkiksi silloin, kun kontaktikulma tai höyrymolekyylin massa on suuri.

Heterogeenista nukleaatiota tutkittiin ilmakeähän olosuhteita vastaavissa olosuhteissa. Kontaktikulmat,jotka vaadittiin, ettei heterogeenista nukleaatiota ole, määritettiin eri olosuhteille ja eri nukleoituville höyryille. Koska θ riippuu höyryn ja yhdinhiukkasen kemiallisista ominaisuuksista ja näiden välisestä vuorovaikutuksesta, tutkittiin lisäksi aerosolin kemiallista kompositiota sekä hiukkasten muodostumisnopeuksia ja kondensaatiohäviötä Pekingissä mitatusta datasta. Toiveissa oli löytää viitteitä siitä, kuinka efektiivinen kondensaatiohäviö ja kemiallinen kompositio mahdollisesti liittyvät toisiinsa. Vahvoja viitteitä tästä ei kuitenkaan vielä löydetty.

Tehottoman heterogeenisen nukleaation vaikutusta efektiiviseen kondensaatiohäviöön tarkasteltiin. Löydettiin useita tilanteita, joissa teoriassa on mahdollista, että tehottomasta heterogeenisesta nukleaatiosta johtuen effektiivinen kondensaatiohäviö on merkittävästi pienempi kuin teoreettinen kondensaatiohäviö. On siis mahdollista, että heterogeenisen nukleaation tehottomuus osaltaan selittää, miksi hiukkasmuodostumistapahtumia havaitaan myös hyvin saastuneissa ympäristöissä.

Avainsanat — Nyckelord — Keywords

Aerosoli, Heterogeeninen nukleaatio, Nukleaatio, Kondensaatiohäviö, Effektiivinen kondensaatiohäviö

Säilytyspaikka — Förvaringsställe — Where deposited

Muita tietoja — Övriga uppgifter — Additional information

Contents

1. Introduction

Aerosol consists of a gas and all the liquid and solid particles that are suspended in it. Our atmosphere is full of these aerosol particles. For example haze and clouds are aerosol. The aerosol particle number concentrations vary from a few dozens per cm^3 in very pristine polar regions [Koponen et al., 2003, Asmi et al., 2010] to tens of thousands per cm^3 [Wu et al., 2008] in polluted mega-cities, and they have many effects on visibility, climate [Ramanathan & Feng, 2009] and human health [Laden et al., 2000]. To be able to understand well all the possible effects of aerosol particles, something which is increasingly important because of climate change and constant urbanization, we need to have a detailed understanding of the processes that influence aerosol populations.

Aerosol particles are usually divided into two categories based on their origin: primary particles and secondary particles. Primary particles are emitted to the atmosphere as particles while secondary particles are formed from vapours by gas-to-particle conversion, such as nucleation, in the atmosphere. They can also be divided based on whether they are from anthropogenic, or human, sources, such as factories or power plants, or natural sources such as emissions from volcanoes or the ocean. In urban areas traffic and industry are examples of large sources of primary aerosol particles. [Seinfeld & Pandis, 2006]

Atmospheric aerosol particles scatter and absorb electromagnetic radiation and influence the radiation balance of Earth [Pöschl, 2005]. They affect how much light hits Earth's surface and how much radiation escapes from the atmosphere. These factors have a considerable effect on climate. In addition to these direct aerosol effects, aerosol particles also have indirect effects through acting as condensation nuclei for clouds and affecting how much clouds there are or what the cloud properties, for example reflectivity, are like [Matheson et al., 2005, Rosenfeld et al., 2014]. Scattering of light from aerosol particles also affects visibility and heavily polluted mega-cities have a largely reduced visibility compared to more pristine areas such as polar regions [Pöschl, 2005].

Aerosol particles can also have multiple significant health effects. Especially those of smaller sizes can enter the human body through the airways and increase inflam-

mation, cause allergic reactions and promote respiratory and cardiovascular diseases [Kim et al., 2015]. There is evidence of increased mortality rates due to air pollution [Kim et al., 2015] and for instance increased lung cancer mortality has been found to correlate with increasing air pollution [Tie et al., 2009].

In the atmosphere vapour molecules collide with each other forming molecular clusters which then grow by condensation of vapours into larger aerosol particles [Zhang et al., 2012]. In the right conditions, such as on a sunny day with photochemical reactions producing sulfuric acid, important precursor gas, in a rather pristine environment, new particle formation events are detected [Zhang et al., 2012]. New particle formation affects strongly how large an effect aerosol particles have on climate by changing the number size distribution and total concentration of aerosol particles and affecting the aerosol composition [Kulmala & Kerminen, 2008, Makkonen et al., 2012]. To accurately predict climate change, the formation of new particles has to be included in models [Makkonen et al., 2012]. The particle number size distribution also matters when considering aerosol health effects. For example it has been observed that the smaller the particles the larger their contribution to cardiovascular diseases is [Franck et al., 2011].

During the evolution of a particle population, many processes affect its number and mass distribution. As mentioned before, vapours condense on particles and the particles can thus grow to larger sizes. Motion, such as Brownian or turbulent motion, causes particles to collide with each other causing them to stick together, which is called coagulation. This causes the total number concentration of particles to go down. The sink of particles by coagulation and vapours by condensation is higher when the concentration of particles is also high such as in polluted environments. [Kulmala et al., 2004b, Pandis et al., 1995]

In theory, high particle concentration should inhibit the formation and growth of new particles because a large fraction of fresh nanoparticles are lost due to coagulation and the vapour concentrations are affected by their condensation sink on those pre-existing particles [Lehtinen et al., 2007]. According to theoretical predictions, there should not be any detectable formation of new particles in very polluted areas. Despite this, observations of new particle formation have been made in heavily polluted environments in China [Kulmala et al., 2017, Xiao et al., 2015]. To explain this, the scavenging of molecular clusters by pre-existing particles needs to be less effective than it is in theory or the particles need to grow faster than is expected. To be able to accurately model evolution of aerosol particle populations and the development of particle number size distributions, we need to be able to explain these observations.

In heterogeneous nucleation vapour molecules nucleate onto a pre-existing surface such as a seed particle, forming a liquid or solid droplet [Lazaridis et al., 1991]. This

thesis explores possible explanations for condensation sink being lower than predicted using heterogeneous nucleation theory and measured data. Special attention is also paid to behaviour of heterogeneous nucleation probability under different conditions. Heterogeneous nucleation probabilities are calculated for different vapours and vapour concentrations and their implications on condensation sink of vapours are considered. Especially the cases with high vapour concentrations and what is needed for there to be no heterogeneous nucleation despite the high vapour concentration are taken into consideration in this thesis. Data from the measurement station of Beijing University of Chemical Technology from winter and spring 2018 is analyzed in addition to theoretical approach. Effect of chemical composition of seed particles is studied along with the effect of the contact angle of heterogeneous nucleation on condensation sink.

2. Theory

2.1 New Particle Formation

In the atmosphere new particles form and grow, if the conditions are right [Kerminen et al., 2018]. In nucleation solid or liquid droplets are formed in a gas phase. In this thesis, the transformation from vapour to liquid is considered. First, a critical cluster, which is a molecular cluster of the size that must be reached for growth to dominate over evaporation, is formed by condensation of vapour molecules. When nucleation is homogeneous, new particles are formed directly from the condensing vapours, but in the case of heterogeneous nucleation vapours condense on surfaces such as pre-existing particles. This is illustrated in Figure 2.1. This saves energy and is more favorable since less surface needs to be formed. Because of this heterogeneous nucleation is considered to dominate over homogeneous in most circumstances. [Kerminen et al., 2018, Vehkamäki, 2006]

It is also possible that molecular clusters form without an energy barrier, and thus not having a critical radius. In such situations the formation of molecular clusters would only be affected by kinetic processes of vapour molecules and particles. [Kulmala et al., 2014] This thesis however focuses on a more traditional view of cluster formation and nucleation.

2.1.1 Homogeneous Nucleation

For particles to form through homogeneous nucleation, the vapour needs to be supersaturated, which means that the saturation ratio is higher than one. The saturation ratio, S, reflects how close to an equilibrium state a vapour in contact with a liquid is, and it is defined as

$$S = p/p_s, \tag{2.1}$$

where p is the partial pressure of vapour and p_s is the saturation pressure of vapour. [Vehkamäki, 2006]

For ideal gas, the partial pressure can be calculated from the general gas equation

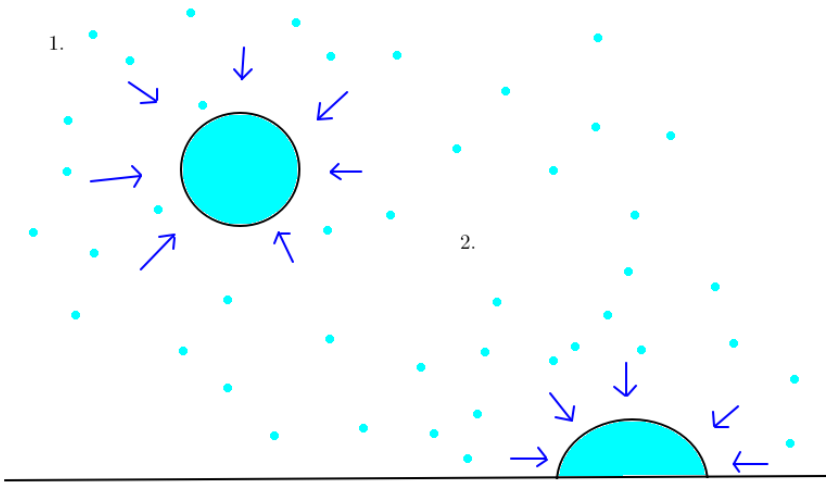

Figure 2.1: 1. Homogeneous nucleation 2. Heterogeneous nucleation on a flat surface

as

$$p = ck_bT, \tag{2.2}$$

where c is concentration of the vapour, T is temperature and k_b is the Boltzmann constant. In this work, the term saturation concentration of vapour is often used. It simply means the vapour concentration that is needed for the saturation rate to equal one.

Considering the most simple case, a situation with a single nucleating vapour, the free energy needed to form a cluster in homogeneous nucleation is

$$\Delta G_{\text{hom}} = n\Delta\mu + A\sigma_{g,l}, \tag{2.3}$$

where $\Delta\mu$ is difference of chemical potentials of vapour and liquid, n is the amount of molecules in the cluster, A is the surface area of the formed droplet and $\sigma_{g,l}$ is surface tension at the interface between the vapour and the forming droplet of liquid. Equation 2.3 takes into account both the energy needed or the energy released by phase transformation and the formation of a droplet. [Vehkamäki, 2006, Lauri, 2006]

Using the ideal gas law, the free energy can be written as

$$\Delta G_{\text{hom}} = 4\pi r^2\sigma_{g,l} - \frac{4}{3}\pi r^3\frac{1}{v}k_bT\ln S, \tag{2.4}$$

where v is volume of a vapour molecule. Critical radius of a cluster is defined as the value corresponding to maximum value of free energy (figure 2.2). From equation 2.4 the critical radius of nucleation is

$$r^* = \frac{2v\sigma_{g,l}}{k_bT\ln S}. \tag{2.5}$$

Now, inserting this to equation 2.3, the energy needed to form a critical cluster for homogeneous nucleation is [Vehkamäki, 2006]

$$\Delta G^*_{\text{hom}} = \frac{4}{3}\pi r^{*2}\sigma_{g,l} \tag{2.6}$$

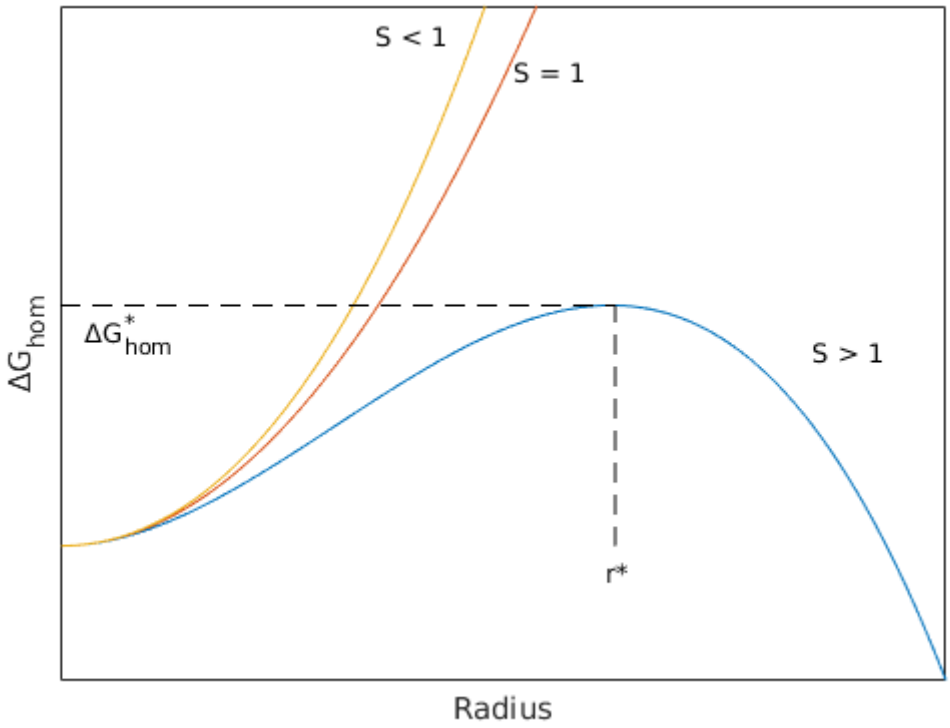

Figure 2.2: Gibbs free energy of homogeneous nucleation for different saturation ratios and radii. With S > 1 a global maximum emerges and the corresponding radius r^* is the critical radius of homogeneous nucleation

2.1.2 Heterogeneous nucleation

The free energy of the formation of a critical cluster in case of heterogeneous nucleation can be calculated from the homogeneous free energy of formation with [Vehkamäki, 2006]

$$\Delta G^*_{\text{het}} = f_g \Delta G^*_{\text{hom}}, \tag{2.7}$$

where f_g is a geometric factor. The geometric factor is related to the ratio between volumes of critical clusters in homogeneous and heterogeneous nucleation. The nucleation free energy needed to form a critical cluster is smaller for heterogeneous nucleation as illustrated in figure 2.3. In the case of nucleation on a flat surface, it equals the ratio of

volumes of critical clusters [Lauri, 2006]. The geometric factor has values in the range $[0, 1]$ and is defined as [Fletcher, 1958]

$$f_g = \frac{1}{2}[1 + (\frac{1 - Xm}{g})^3 + X^3(2 - 3\frac{(X - m)}{g} + (\frac{X - m}{g})^3) + 3X^2m(\frac{X - m}{g} - 1)], \quad (2.8)$$

where

$$g = \sqrt{1 + X^2 - 2Xm} \quad (2.9)$$

and X is the ratio of radius of the seed particle and the critical radius,

$$X = R_{seed}/r^*. \quad (2.10)$$

Contact parameter m is

$$m = \cos\theta, \quad (2.11)$$

where θ is a contact angle (figure 2.12).

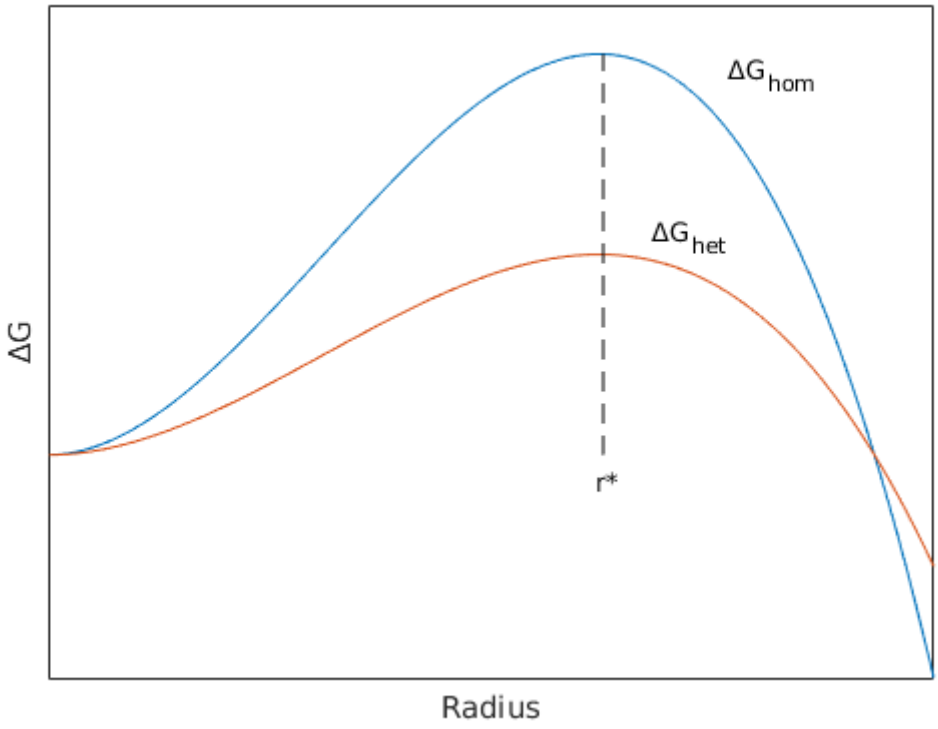

Figure 2.3: Formation free energy in homogeneous versus heterogeneous nucleation. r^* is the critical radius of nucleation.

The contact angle θ of heterogeneous nucleation is related to the surface energy of the condensing droplet. The smaller the contact angle, the less energy is needed to form a droplet. When $\theta = 0°$, the surface is completely wettable and when $\theta = 180°$, the droplet and surface are completely separate and the situation corresponds

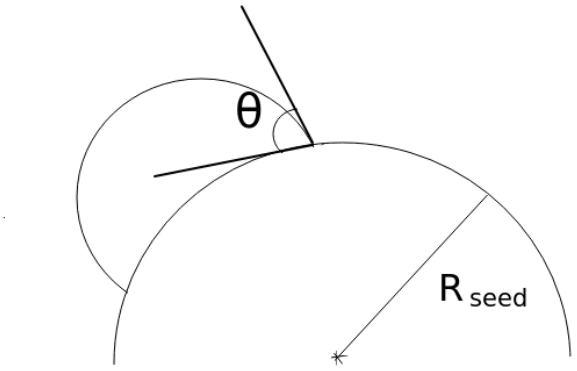

Figure 2.4: Contact angle θ for nucleation on a spherical seed particle.

to homogeneous nucleation. Young's equation relates the inter-facial tensions to each other. It is [Lazaridis, 1991]

$$\cos\theta = \frac{\sigma_{g,seed} - \sigma_{l,seed}}{\sigma_{g,l}}, \tag{2.12}$$

where θ is the contact angle, $\sigma_{g,seed}$ is the surface tension of the thin film remaining on surface of this body and $\sigma_{l,seed}$ is the surface tension between the seed particle and the forming droplet.[Lazaridis, 1991]

The values for the contact angle can be quite different depending on the vapour and composition of the nucleation surface. For example for n-propanol, the contact angle is 43° on teflon, but only 7° on polyethylene. For water contact angle of heterogeneous nucleation is 110° on paraffin and 86° on graphite. Clearly the chemical composition of the seed particle has a very large effect on what the contact angle will be for different vapours. [Butt et al., 2003]

2.1.3 Nucleation Probability

In the case of heterogeneous nucleation, unlike in homogeneous nucleation, the nucleation rate is hard to measure directly. Instead, the proportion of activated aerosols, or the nucleation probability, is considered [Lauri, 2006]. Nucleation probability can then be expressed as $P_{\text{het}} = \frac{N_{activated}}{N_{total}}$ where $N_{activated}$ is the number of activated particles and N_{total} is the total number of particles. A particle is considered activated if

vapours have condensed on it. Nucleation probability depends on the rate of heterogeneous nucleation. Nucleation rate for heterogeneous nucleation in one-component case is [Lazaridis et al., 1991]

$$J_{\text{het}} = \beta Z N_{ads} \exp\left\{\left(\frac{-\Delta G^*_{\text{het}}}{k_b T}\right\}\right), \tag{2.13}$$

where β is the growth rate of the nucleus. It is defined as [Pruppacher, 1998]

$$\beta = \frac{p}{\sqrt{2\pi k_b T m}}. \tag{2.14}$$

Now p is the partial pressure of the condensing vapour and m is the mass of a vapour molecule. Zeldovich correction factor Z is approximated with the value for homogeneous nucleation and it is [Lazaridis et al., 1991]

$$Z = \frac{v}{2\pi r^{*2}} \sqrt{\frac{\sigma_{g,l}}{k_b T}}, \tag{2.15}$$

where v is the volume of a vapour molecule. Concentration of vapour molecules on the surface of the forming droplet is [O'Dowd & Wagner, 2007]

$$N_{ads} = \frac{S p_s}{\sqrt{2\pi m k_b T}} \frac{1}{\upsilon} \exp\left\{\left(\frac{L}{k_b T}\right)\right\}, \tag{2.16}$$

where υ is the vibration frequency of a vapour molecule and L is the latent heat of vaporization per molecule.

Probability for heterogeneous nucleation to occur in a given time-span t is [Lazaridis et al., 1992]

$$P_{\text{het}} = 1 - \exp\left\{\left(-J_{\text{het}} 4\pi R^2_{seed} t\right)\right\}. \tag{2.17}$$

Often, the onset of heterogeneous nucleation is considered to be the nucleation probability of 0.5 and the corresponding saturation ratio. This is also used in this thesis as the onset of heterogeneous nucleation when defining whether heterogeneous nucleation is effective or not.

2.2 Survival Probability

Atmospheric particle populations include particles from a wide size range and are affected by many processes between particles of similar or different sizes. The probability that a growing particle ever grows to a defined larger size is called its survival probability. Usually the survival probability is considered for small freshly nucleated particles and their growth to larger sizes.

2.2.1 Kerminen-Kulmala Equation

If the smaller particles of diameter d_2 have a formation rate of J_2, it is theoretically related to the formation rate of larger particles with diameter d_1 according to Kerminen-Kulmala [Kerminen & Kulmala, 2002]

$$J_2 = J_1 \exp\left\{[0.23\frac{\mathrm{CS}'}{\mathrm{GR}'}(\frac{1\mathrm{nm}}{d_1} - \frac{1\mathrm{nm}}{d_2})]\right\}, \tag{2.18}$$

where $\mathrm{CS}' \approx \mathrm{CS}/(10^{-4}\mathrm{s}^{-1})$ and $\mathrm{GR}' = \mathrm{GR}/(1\,\mathrm{nmh}^{-1})$. $\frac{\mathrm{CS}'}{\mathrm{GR}'}$ can be defined as a dimensionless survival parameter P [Kulmala et al., 2017] and the larger it is, the smaller the probability, which can be expressed as J_1/J_2, of particles growing to diameter of d_1 is. This probability is the previously mentioned survival probability.

CS is the condensation sink and it will be discussed in the next subsection. GR is the growth rate of the particles in the size range [d_1,d_2]. It is defined as the change of diameter per time. GR is

$$\mathrm{GR} = \frac{\Delta d_{12}}{\Delta t_{12}}, \tag{2.19}$$

where Δd_{12} is the difference between diameters d_1 and d_2 and Δt_{12} is the time it takes for a particle to grow from d_2 to d_1. The faster the particle grows, the larger the probability of it surviving to larger sizes will be.

2.2.2 Condensation Sink

Condensation sink CS of particles tells how fast vapour molecules that could potentially partake in formation of new particles condense on pre-existing particles. In the equation 2.18 condensation sink in reality is a replacement for the coagulation sink, which tells how fast particles disappear by colliding and sticking to larger particles and it can be expressed in terms of the condensation sink [Kerminen & Kulmala, 2002]. A smaller condensation sink favors particle growth since less of them is scavenged by pre-existing particles.

The condensation sink is [Pirjola et al., 1999]

$$\mathrm{CS} = 2\pi D \sum_i \beta_i d_i N_i, \tag{2.20}$$

where D is the diffusion constant of the vapour, d_i is diameter of particle i, β is the transitional correction factor and N_i the concentration. Condensation sink thus depends on the particle size number distribution. If the particle number size distribution is measured and the vapour properties are well known, the condensation sink can be calculated from it.

It has been argued that the survival parameter P has to be smaller than 50 for new particle formation to occur [Kulmala et al., 2017]. However, it has been observed that in China new particle formation frequently takes place in very polluted mega-cities where the survival parameter can be as high or even higher than 200 [Kulmala et al., 2017]. Observations of formation rates strongly disagree with theoretical expectations when survival parameter is large. To explain this, the actual survival parameter and thus either the condensation sink needs to be lower or the growth rate larger than measured values.

It is possible that not all vapour molecules that collide with a particle stick to it. This could be equated to the heterogeneous nucleation being improbable for certain vapours and seed particles. Condensation sink in equation 2.18 can be replaced by an effective condensation sink producing smaller values of survival parameter and larger values of survival probability. The effective condensation sink is

$$\mathrm{CS}_{\mathrm{eff}} = \beta \times \mathrm{CS}, \tag{2.21}$$

where β is the ratio between molecules that stick to the total number of molecules.

In this thesis the implications of improbable heterogeneous nucleation to the effective condensation sink are considered. Values for effective sink are calculated assuming that the effective sink is smaller because particles with diameters under a certain minimum diameter do not partake in condensation sink because for them heterogeneous nucleation is not effective anymore.

3. Methods

3.1 Measurements and Data Analysis

Measured data was used and analyzed in this thesis to supplement a more theoretical approach. The measurements were done at the measurement station of Beijing University of Chemical Technology (39°56'31"N,116°17'50"E, Beijing) between January 17 December 02 in 2018. The measurement site was located in urban area and close to traffic emissions. The measurement instruments used are described in Table 3.1.

The measured values that were used in this thesis are

- Formation rate of 1.5 nm-particles, $J_{1.5}$
- Formation rate of 3 nm-particles, J_3
- Condensation sink CS
- Growth rate GR
- Particle number size distribution
- Aerosol chemical composition
- Trace gas concentrations

Formation rate $J_{1.5}$ was calculated from particle size distributions measured using a Particle Size Magnifier (PSM) and the formation rate J_3 using Neutral Cluster and Air Ion Spectrometer (NAIS). They were calculated alongside condensation sink with methods according to Kulmala et al. (2012). The growth rates were determined from NAIS data using the appearance time method [Kulmala et al., 2012, Lehtipalo et al., 2016]. The particle number size distribution was measured with Scanning Mobility Particle Sizer (SMPS). Chemical composition was measured with Aerosol Chemical Speciation Monitor, or ACSM. The compounds that could be measured with ACSM and their abbreviations used later in this thesis are in Table 3.4. Gas-phase pollutant concentrations of CO and NOx were measured with Thermo Environmental Instruments.

To maximize the amount of data, growth rate of 2.9 nmh^{-1} was used to calculate particle formation rates when growth rate could not be determined. Survival probability was calculated for particles growing from 1.5 nm to 3 nm as $J_3/J_{1.5}$ according to equation 2.18. The survival parameter was calculated using that same equation. This was done for median values for every half an hour between 9:00 and 14:00. The median values of mass fractions and mass concentrations of different chemical compounds measured with ACSM were also included to see whether they had an influence on the values of survival probability in relation to the survival parameter. This could give implications about the possible dependency of the effective condensation sink on particle composition.

Table 3.1: Instruments used in measuring the data used.

Instrument	Measured Quantity	Working principle	
NAIS	Total concentration of air ions and neutral particles in size range 2.5-42 nm and ions in size range 0.8 nm-42 nm	Particles are charged, unless ions are measured, in well-defined conditions with a unipolar charge so that the charge distribution is known and thee detection of particles happens electrically based on their electric mobility.	[Mirme & Mirme, 2013]
PSM	Concentration of nanoparticles in size range 1.2-2.5 nm	Cooled aerosol sample flow is mixed with heated clean air saturated by a working fluid, which is diethylene-glycol, creating supersaturated surroundings, which makes particles grow by condensation. The particles are then counted by a Condensation Particle Counter	[Vanhanen et al., 2011]
SMPS	Number size distribution in size range 3 nm - 10 µm	Particles are classified according to their electrical mobility and the electric field is scanned continuously selecting particles of certain size after which their concentration is calculated	[Wang & Flagan, 1990]
ACSM	Mass and chemical composition of PM2.5	Aerosol sample is thermally vaporized and analyzed by a quadrupole mass spectrometer	[Ng et al., 2011]

Table 3.2: Abbreviations of chemical compounds measured by ACSM

HOA	Primary Organic Traffic Exhaust
COA	Cooking Organic Emissions
CCOA	Coal Combustion Organic Emissions
BBOA	Biomass Burning Organic Emissions
OOA	Secondary Organic Aerosol
NH4	Ammonium
NO3	Nitrate
SO4	Sulphate
Chl	Chloride
BC	Black Carbon

3.2 Heterogeneous Nucleation Model

Heterogeneous nucleation probabilities were calculated according to Classical Nucleation Theory introduced in section 2 . Many different situations were considered and variables such as mass of molecule, surface tension of the liquid-vapour interface, saturation concentration, vapour concentration and the radius of seed particle were all varied. All the situations were assumed to be unary, which means that the nucleating vapour consisted of one type of molecules or molecular clusters, and there was no involvement of for example water vapour.

Values that were always kept constant in the calculations are presented in Table 3.3. It was assumed that in practice these values would be close enough for different species as to not make a significant difference in the nucleation probability. This was tested by calculating the contact angle corresponding to onset of heterogeneous nucleation for five times larger vibration frequency υ, which produced less than a percent of difference in nucleation probability, and for a latent heat of $L = 9.0 \times 10^{-20}\,\mathrm{J/molecule}$ which resulted in about three percent difference compared to when a value of $8.0 \times 10^{-20}\,\mathrm{J/molecule}$ is used.

Table 3.3: Values kept constant used for modelling of heterogeneous nucleation

Quantity	Symbol	Value
Time	t	$100\,\mathrm{ms}$
Temperature	T	$278.15\,\mathrm{K}$
Latent heat	L	$8.0 \times 10^{-20}\,\mathrm{J/molecule}$
Vibration frequency	υ	$1 \times 10^{12}\,1/\mathrm{s}$

Unless otherwise specified, such as when studying an organic vapour, the value used for surface tension was $0.055\,\mathrm{N/m}$, which approximately corresponds to the value for sulfuric acid. Similarly, the mass and volume of vapour molecules were chosen to be that of sulfuric acid, $m = 98\,\mathrm{u}$ and density $\rho = 1830\,\mathrm{kgm^{-3}}$, unless for example the effect of vapour molecule size on heterogeneous nucleation was investigated. [Haynes, 2014] The situations investigated are presented in Table 3.4.

Values close to properties of sulfuric acid were used because it has been observed that sulfuric acid is an important species in new particle formation [Kirkby et al., 2011, Kulmala et al., 2004b]. Vapour concentrations used were between $5 \times 10^6\,\mathrm{cm^{-3}}$ and $2 \times 10^7\,\mathrm{cm^{-3}}$ because this thesis concentrates on highly polluted areas in China where sulfuric acid concentrations can reach over $1 \times 10^7\,\mathrm{cm^{-3}}$ [Yao et al., 2018].

The variable of interest was the nucleation probability (equation 2.17) and how

Table 3.4: Different cases heterogeneous nucleation probabilities were calculated for.

	Investigated	c (cm^{-3})	c_{sat} (cm^{-3})	σ (N/m)	m (u)
1	Dependency of HN on SA vapour concentration and saturation concentration	1×10^6 - 2×10^7	5×10^4 - 5×10^5	0.055	98
2	Dependency of HN on surface tension	1×10^7	1×10^5 & 5×10^5	0.02 - 0.08	98
3	Dependency of HN on molecule mass and size	1×10^7	5×10^5	0.055	60-600
4	HN of SA-DMA clusters	1×10^7 & 2×10^7	1×10^5	Calculated using equation 3.2	Calculated using equation 3.1
5	HN of LVOC clusters	5×10^7 - 2×10^8	3×10^6	0.02	(Number of LVOC molecules) $\times$ 203

it changed for different values of the contact angle (equation 2.12) and seed particle diameter. The requirements for there to be no heterogeneous nucleation were investigated for different situations. The minimum contact angles, θ_{min}, for heterogeneous nucleation to be ineffective on the seed particle were determined using the contact angles corresponding to the nucleation probability of 0.5. It should be noted that the results in this thesis are not always directly applicable to real-life situations because of lack of information on contact angles for different combinations of vapour and seed particle composition.

Cases with clusters composed of sulfuric acid and dimethylamine, or DMA, molecular clusters and low-volatile organic compound, or LVOC, molecular clusters were also considered. The clusters considered were chosen because of their likely participation in new particle formation [Kulmala et al., 2014]. The properties used for sulfuric acid, dimethylamine and model LVOC molecule are presented in Table 3.5 and they were chosen so that they corresponded to real values. For dimethylamine molecular mass of 45 u, surface tension of 0.026 N/m and density of 650 kg/m^3 were used

[Haynes, 2014]. For low-volatile organic compounds,f or LVOC saturation concentration of $3 \times 10^6\,\mathrm{cm}^{-3}$, surface tension of $0.02\,\mathrm{N/m}$, molar volume of exemplary molecule $135.5\,\mathrm{cm}^3\mathrm{mol}^{-1}$ [Kulmala et al., 2004a] corresponding to molecular mass of 203 u, and density of $1500\,\mathrm{kgm}^{-3}$ [Ehn et al., 2014] were used.

For clusters of dimethylamine and sulfuric acid, density was calculated as

$$\rho = (N_{SA} \times \rho_{SA} + N_{DMA} \times \rho_{DMA})/(N_{SA} + N_{DMA}) \tag{3.1}$$

and surface tension as

$$\sigma = (N_{SA} \times \sigma_{SA} + N_{DMA} \times \sigma_{DMA})/(N_{SA} + N_{DMA}), \tag{3.2}$$

where N_{SA} and N_{DMA} are number of molecules of sulfuric acid and dimethylamine respectively.

Table 3.5: Properties of different chemical species used in calculations of heterogeneous nucleation.

Species	Quantity	Value
Sulfuric Acid	m_{SA}	98 u
	σ_{SA}	$0.055\,\mathrm{N/m}$
	ρ_{SA}	$1830\,\mathrm{kgm}^{-3}$
Dimethylamine	m_{DMA}	45 u
	σ_{DMA}	$0.026\,\mathrm{N/m}$
	ρ_{DMA}	$650\,\mathrm{kgm}^{-3}$
LVOC	v_{LVOC}	$135.5\,\mathrm{cm}^3\mathrm{mol}^{-1}$
	σ_{LVOC}	$0.02\,\mathrm{N/m}$
	ρ_{LVOC}	$1500\,\mathrm{kgm}^{-3}$

Effect of hydrates, or electric charge, are not taken into account in this thesis. However, including hydrates would make the nucleation rates, and thus the nucleation probabilities, at least somewhat lower [Lazaridis, 1991]. Including ionization in the calculations would enhance enhance heterogeneous nucleation and make the nucleation probabilities higher especially for smaller particles [Winkler et al., 2008].

3.3 Condensation Sink Analysis

Condensation sinks were determined from measured particle number size distributions in Beijing according to the equation 2.20. A median condensation sink was calculated from the number size distributions for days when new particle formation events were detected and for between 9 and 11 in the morning. The median particle size distribution

for this time-span is shown in Figure 3.1. The smallest particles are the most abundant and there are few particles with diameters close to or over 1 µm.

Effective condensation sinks were calculated similarly to the actual condensation sink, but assuming a minimum size for particles participating in sink. Particles with this diameter, or smaller, were assumed to not cause any sink because of ineffective heterogeneous nucleation. The ratios of these effective condensation sinks to the condensation sink for different minimum diameters are seen in Figure 3.2. It can be observed that to have a significant effect on the condensation sink, the minimum diameter has to be tens of nanometers. This is because even though the smallest particles are the most abundant they rarely collide with vapour molecules because of their smaller surface and collision areas.

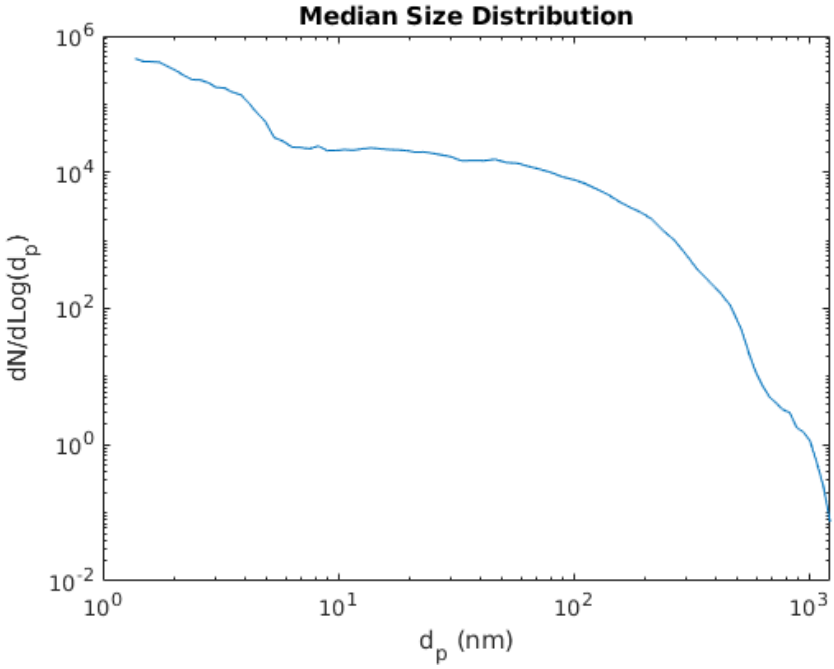

Figure 3.1: Median number size distribution between 9 and 11 in the morning in a day with new particle formation event

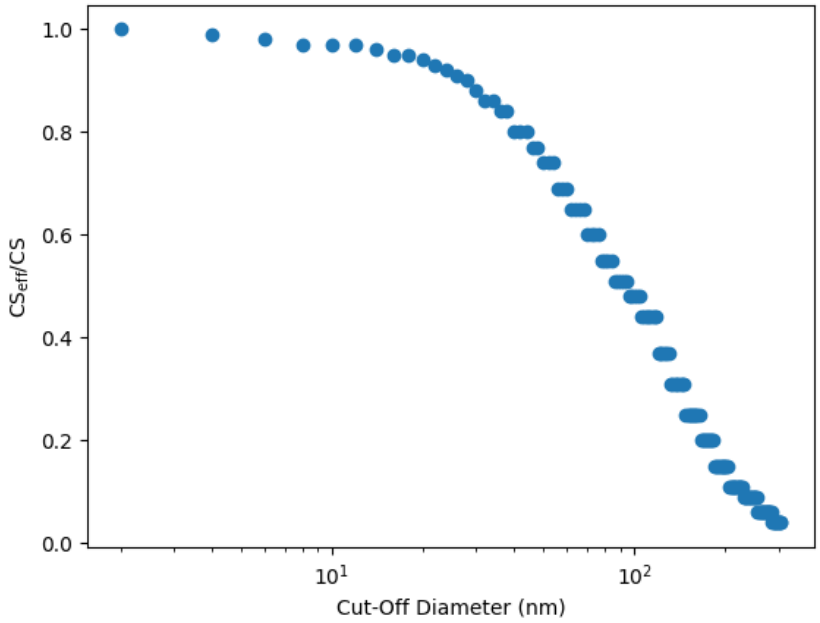

Figure 3.2: The ratio of condensation sink and effective condensation sink for different minimum diameters for particle to effectively participate in condensation sink

4. Results

4.1 Magnitude of Formation Rates J_3 and $J_{1.5}$

Figure 4.1 shows the median diurnal cycle of formation rate of 3 nm particles, J_3, and formation rate of 1.5 nm particles, $J_{1.5}$, on new particle formation event days. It can be seen that the formation rate J_3 is on an average new particle formation day unexpectedly large compared to the formation rate of 1.5 nanometer particles. On a median NPF day at 12:00 $J_{1.5} \approx 1 \times 10^2\,\mathrm{cm^{-3}s^{-1}}$ and $J_3 \approx 7 \times 10^1\,\mathrm{cm^{-3}s^{-1}}$. The formation rate of larger particles should be much smaller than smaller particles because of the coagulation to the pre-existing particle population, which is especially significant in the polluted urban environment. The emissions of 3 nm particles from traffic exhaust could possibly explain this. It has been observed that traffic is a significant source of sub-3 nm particles [Rönkkö et al., 2017].

Figure 4.2 shows how survival probability depended on the survival parameter (equation 2.18). It can be seen that the survival probability is smaller for a higher survival parameter as equation 2.18 predicts. It can also be seen that, as mentioned before, J_3 is surprisingly close to $J_{1.5}$ and is in some days actually larger than $J_{1.5}$, which could be because of traffic emissions of sub-3 nanometer particles. There is not a single value with a survival probability below 0.1. In theory for a survival parameter of 50 the survival probability from 1.5 nm to 3 nm particle should be 0.02 and for a survival parameter of 500 the survival probability should be so close to zero that the growth of particles to size of 3 nm should be practically impossible [Kulmala et al., 2017]. The values in Figure 4.2 are very different compared to what theory predicts.

In Figure 4.3 the particle size distribution, formation rates and also mass concentrations of CO and NO_x, because they are largely a result of traffic emissions, during one day are plotted. Starting after 09:00 emergence and following growth of new particles can be seen from the upper panel. This is accompanied by slight rise in J_3 (middle panel) and clear decline in CO and NO_x concentrations (lower panel). Multiple similar daily plots were made. However a correlation between traffic exhaust and J_3 could not be seen based on them.

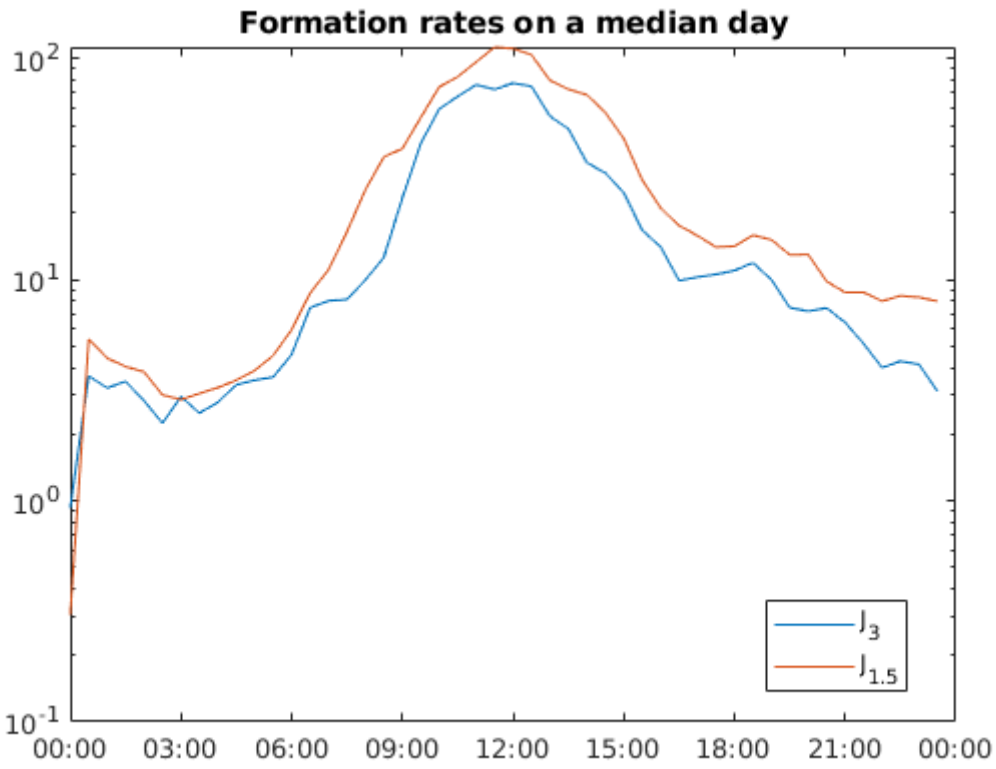

Figure 4.1: Formation rates J_3 and $J_{1.5}$ particles during a median new particle formation event day in Beijing.

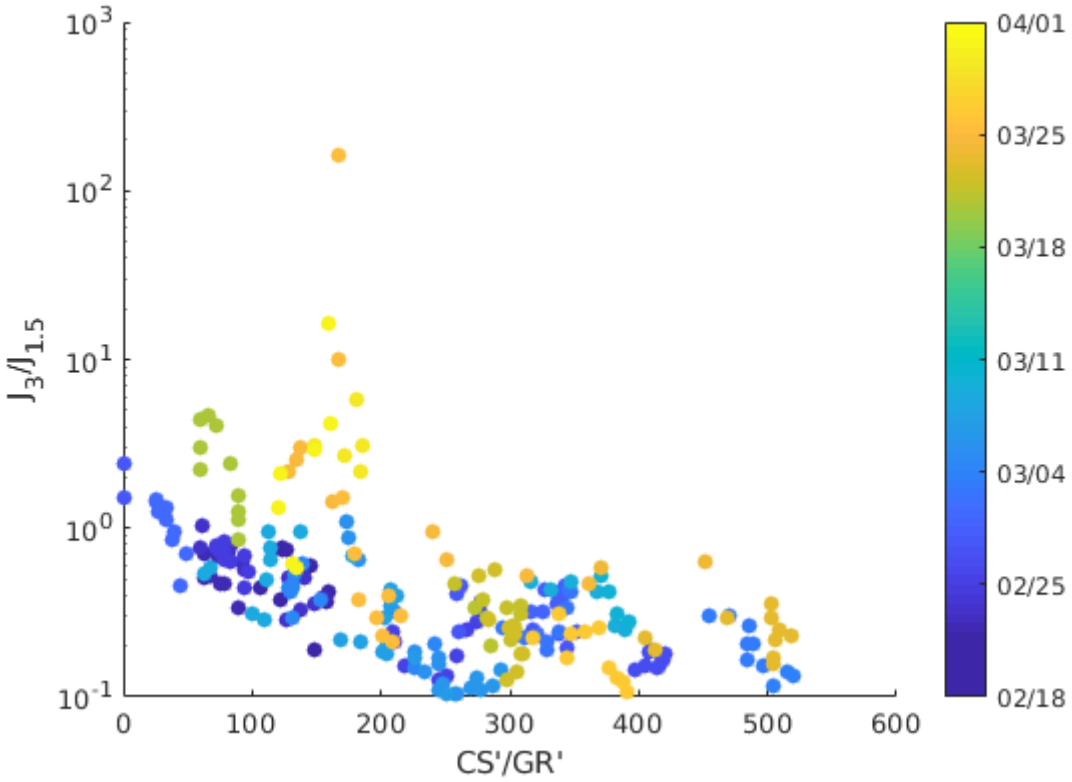

Figure 4.2: Survival probability as a function of survival parameter in Beijing (equation 2.18). The colour reflects the date the values were measured in.

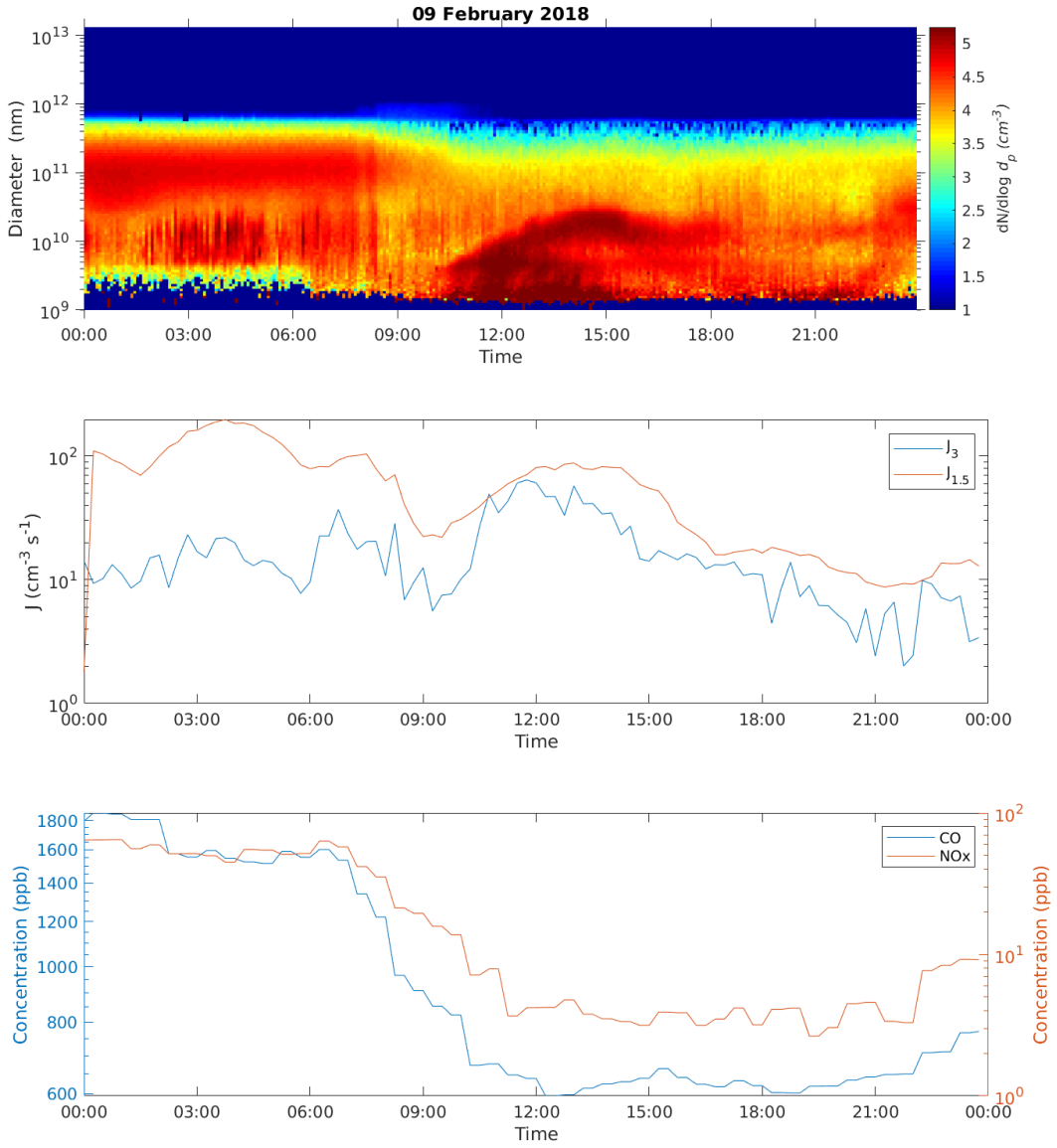

Figure 4.3: Data from 09.02.2018 in Beijing. In the first panel from the top there is the particle number size distribution during a particle formation event day. In the second there are the corresponding formation rates J_3 and $J_{1.5}$. In the third one there are the concentrations of CO and NOx during the day.

4.2 Effect of Particle Chemical Composition on Particle Survival Probability

It was investigated how the ratio of survival probability and survival parameter depended on chemical composition of particulate matter. This ratio should remain same (equation 2.18), but it was observed to vary from below 10^{-3} to 1. This could be at least partially because of the effective condensation sink being different from the condensation sink (equation 2.21).

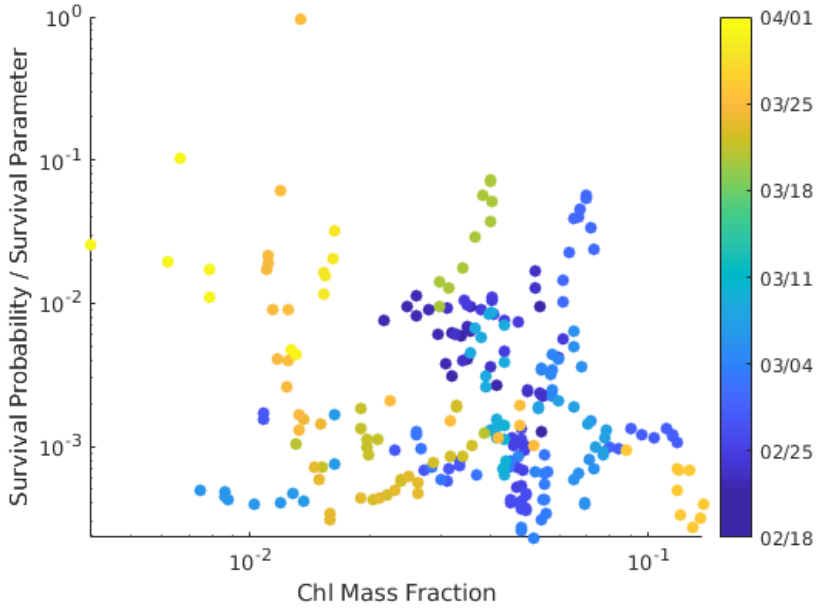

Figure 4.4: Ratio of survival probability and survival parameter and the corresponding aerosol mass fraction of chloride during different days in Beijing.

From Figure 4.4 we can see that there does not seem to be a clear correlation between mass fraction of chloride Chl in the particles and the ratio of survival probability and survival parameter. Therefore chloride content of the particles does not seem to have an influence on the magnitude of the effective condensation sink. Similar observations can be made for mass fractions of sulfate SO4 (Figure 4.5) nitrate NO3 (Figure 4.6), ammonium NH4, (Figure 4.7) and biomass burning organic emissions BBOA (Figure 4.8). There seems to however be a weak negative correlation between the ratio of survival probability and survival parameter and mass fractions of cooking organic emissions COA (Figure 4.9), black carbon BC (Figure 4.10) and possibly also primary organic traffic exhaust HOA (Figure 4.11) and coal combustion organic emissions CCOA (Figure 4.12). This could mean that large mass fractions of these chemical compounds in aerosol would result in a small effective condensation sink. Secondary

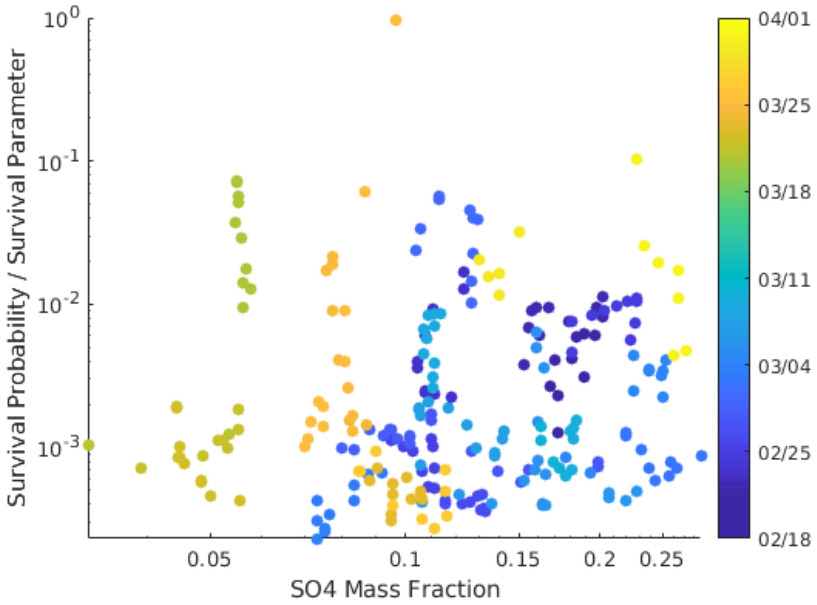

Figure 4.5: Ratio of survival probability and parameter and the corresponding aerosol mass fraction of sulphate during different days in Beijing..

organic aerosol OOA mass fraction shows a possible weak positive correlation as seen from Figure 4.13.

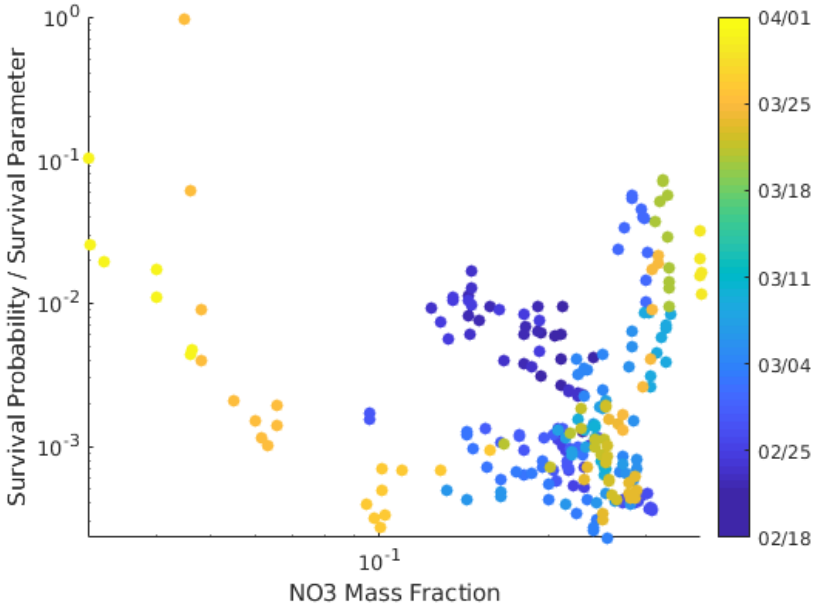

Figure 4.6: Ratio of survival probability and parameter and the corresponding aerosol mass fraction of nitrate during different days in Beijing..

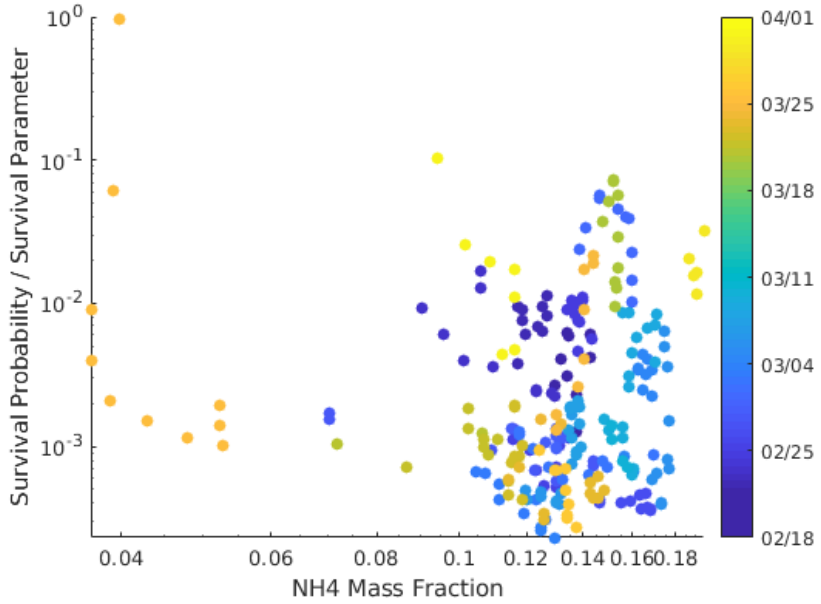

Figure 4.7: Ratio of survival probability and parameter and the corresponding aerosol mass fraction of ammonium during different days in Beijing..

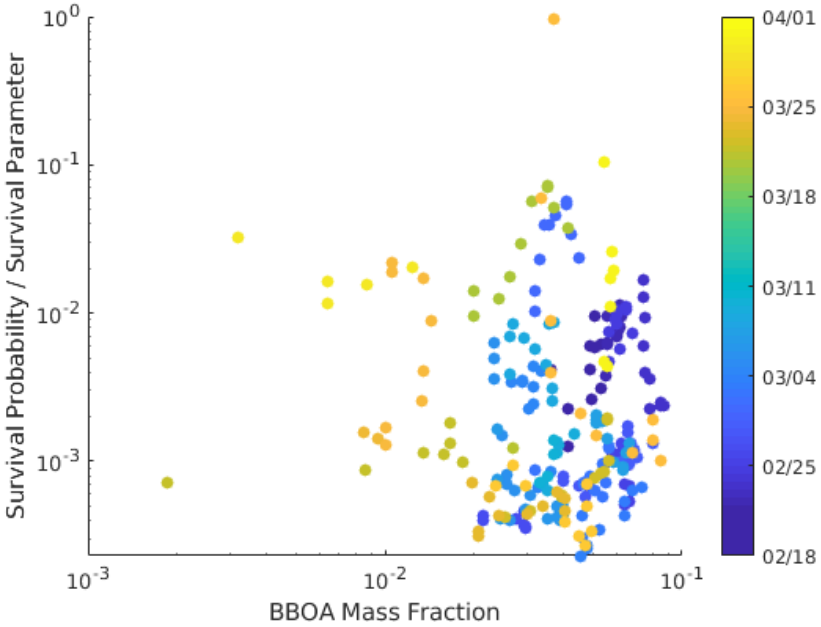

Figure 4.8: Ratio of survival probability and parameter and the corresponding aerosol mass fraction of biomass burning organic emissions during different days in Beijing..

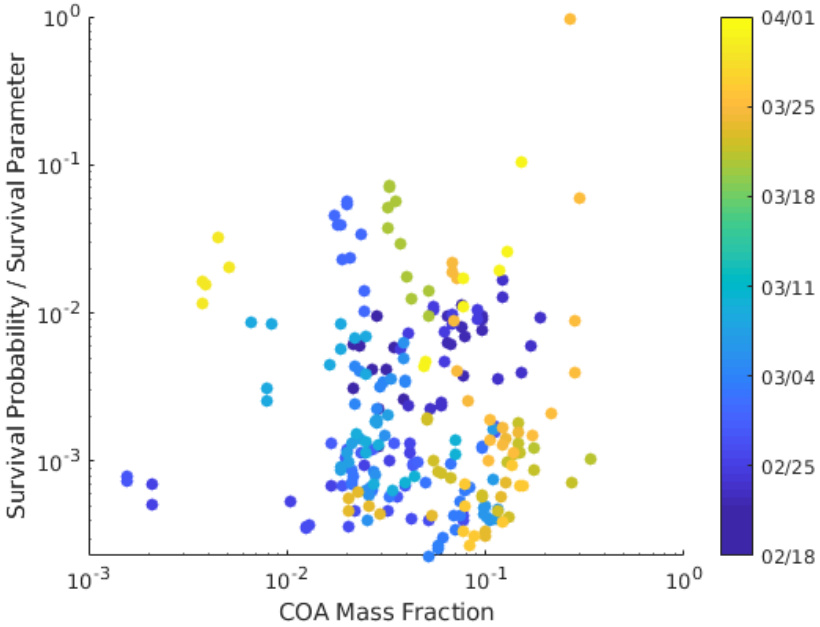

Figure 4.9: Ratio of survival probability and survival parameter and the corresponding aerosol mass fraction of cooking organic exhaust during different days in Beijing.

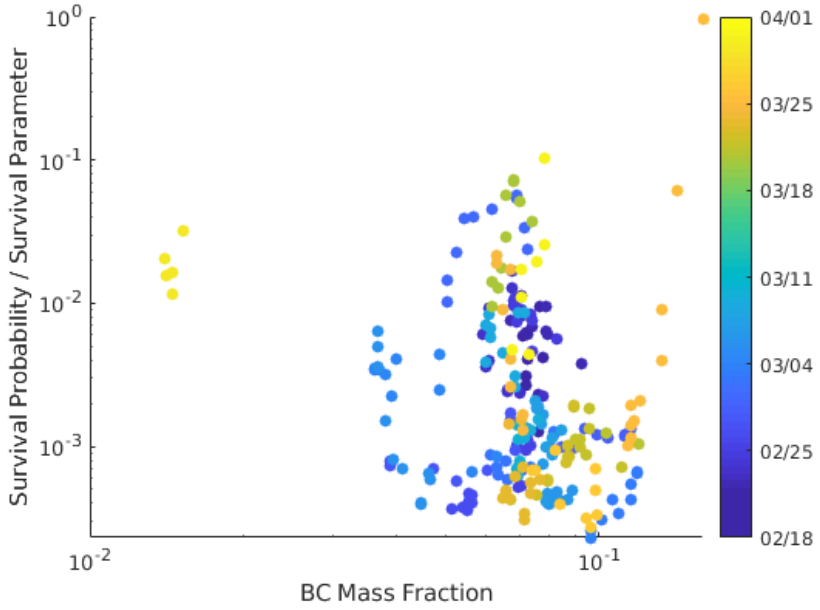

Figure 4.10: Ratio of survival probability and parameter and the corresponding aerosol mass fraction of black carbon during different days in Beijing.

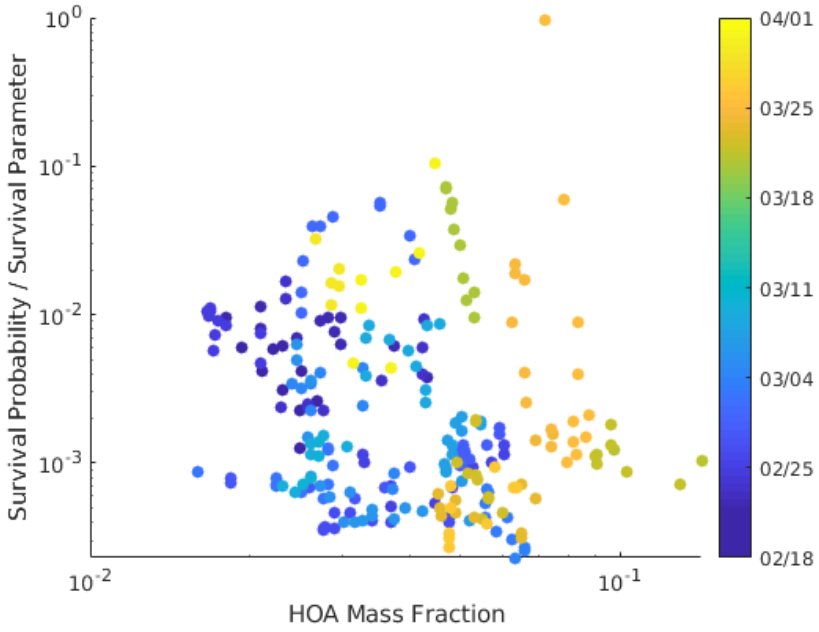

Figure 4.11: Ratio of survival probability and parameter and the corresponding aerosol mass fraction of hydrocarbon-like organic aerosol during different days in Beijing.

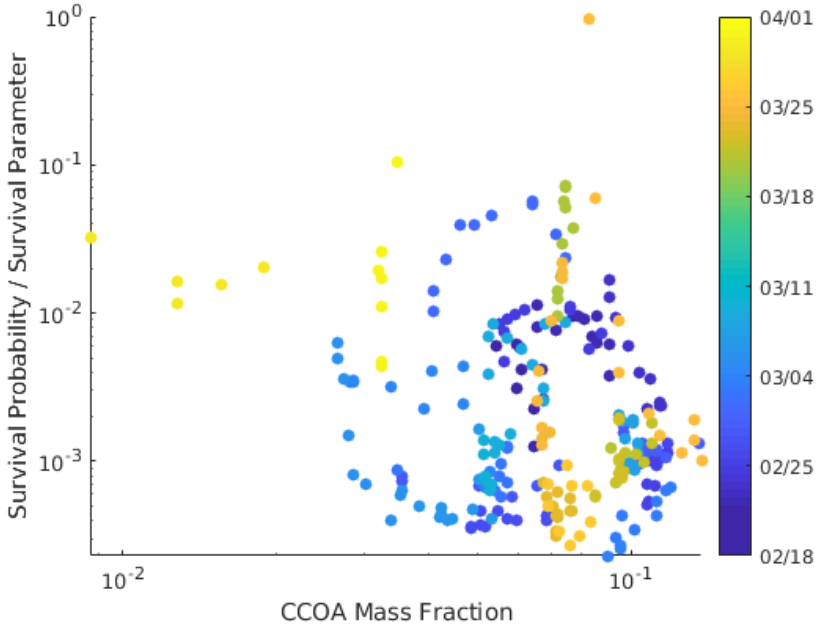

Figure 4.12: Ratio of survival probability and parameter and the corresponding aerosol mass fraction of coal combustion organic emissions during different days in Beijing..

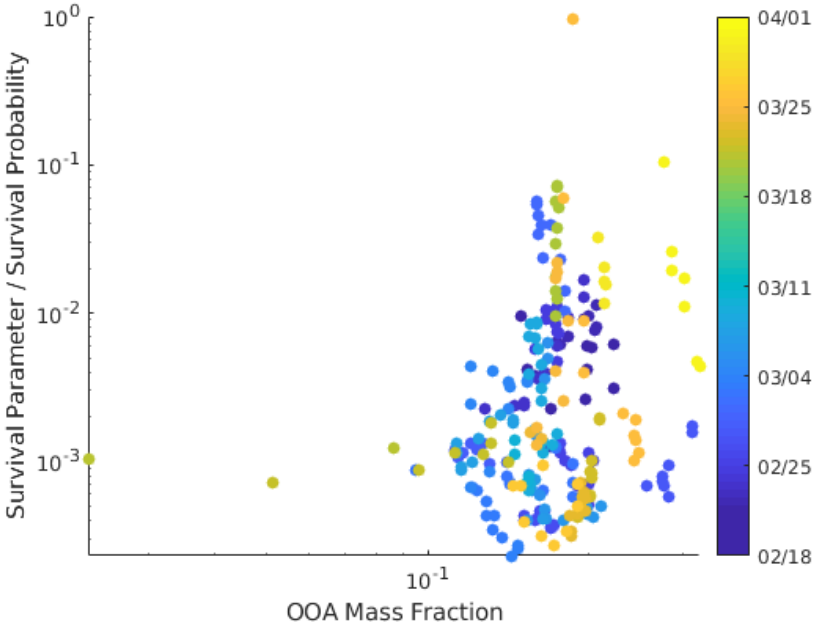

Figure 4.13: Ratio of survival probability and parameter and the corresponding aerosol mass fraction of secondary organic aerosol during different days in Beijing..

To investigate the dependency of ratio of survival probability and survival parameter on chemical composition deeper, correlation coefficients and P-values were calculated for logarithms of base 10 of the ratio and chemical compound mass fraction. These values are in Table 4.1. There is a weak but statistically significant negative correlation between measured HOA, COA, CCOA, and black carbon mass fractions and the ratio of survival probability and survival parameter. It is possible that large fractions of these chemical compounds might be connected to a small effective condensation sink. However no strong indications on a connection was yet found and it cannot conclusively be said that the chemical composition has any significant effect on effective condensation sink.

Table 4.1: Correlation coefficients R and P-values for logarithms of mass fraction and ratio of survival probability and survival parameter.

Compound	R	P
Primary Organic Traffic Exhaust HOA	-0.2612	3×10^{-5}
Cooking Organic Emissions COA	-0.2129	0.0007
Coal Combustion Organic Emissions CCOA	-0.2575	4×10^{-5}
Biomass Burning Organic Emissions BBOA	-0.0479	0.4503
Secondary Organic Aerosol OOA	0.2188	0.0005
Ammonium NH4	0.0106	0.8669
Nitrate NO3	-0.0843	0.1824
Sulphate SO4	0.1374	0.0292
Chloride Chl	-0.1499	0.0173
Black Carbon BC	-0.2641	2×10^{-5}

4.3 Heterogeneous Nucleation

4.3.1 Dependency of Heterogeneous Nucleation on Contact Angle

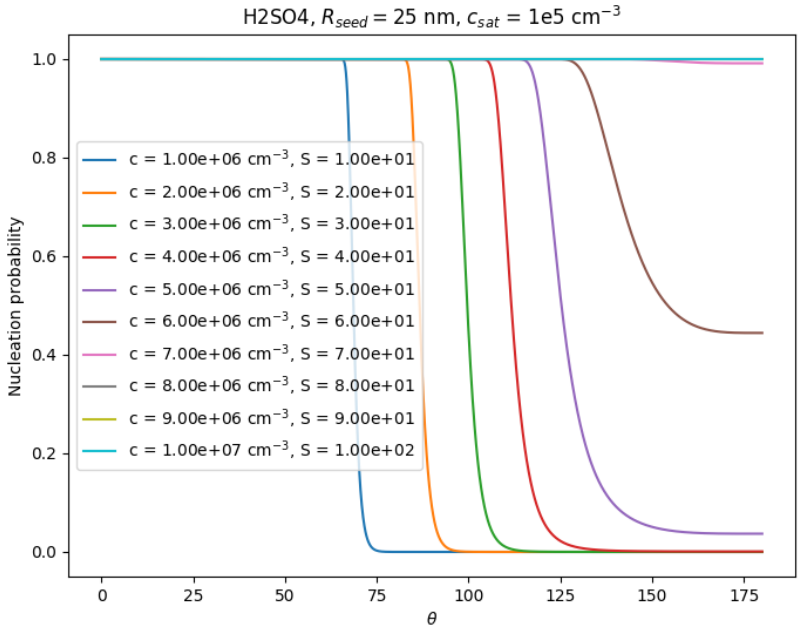

(a) Radius of seed particle is 25 nm.

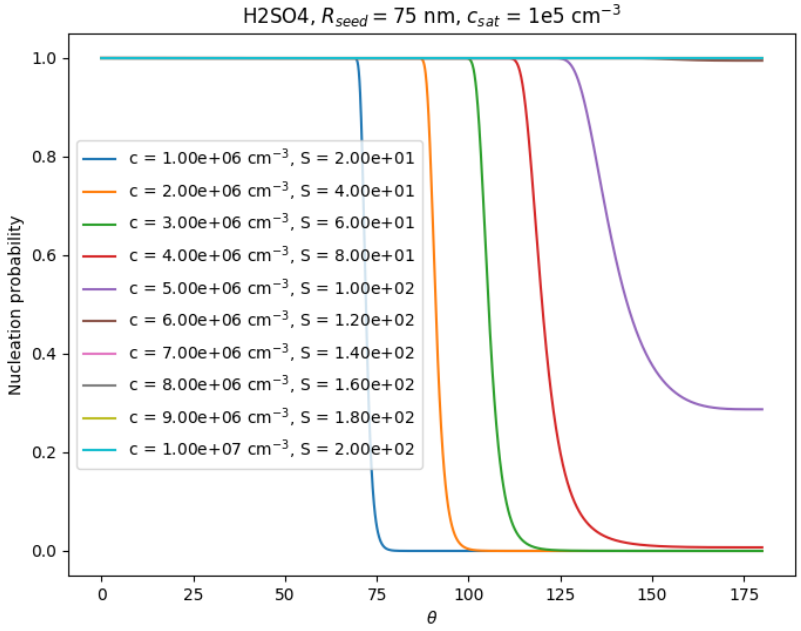

(b) Radius of seed particle is 75 nm.

Figure 4.14: Dependency of nucleation probability on contact angle θ for sulfuric acid when vapour concentration is between 1×10^6 cm^{-3} and 1×10^7 cm^{-3} and saturation concentration is 1×10^5 cm^{-3}.

Heterogeneous nucleation probabilities (equation 2.17) were calculated for different contact angles between 0° and 180°, sulfuric acid vapour concentrations between $1 \times 10^6\,\mathrm{cm}^{-3}$ and $2 \times 10^7\,\mathrm{cm}^{-3}$ and saturation concentrations of a sulfuric acid vapour between $5 \times 10^4\,\mathrm{cm}^{-3}$ and $5 \times 10^5\,\mathrm{cm}^{-3}$. As seen from Figure 4.14, heterogeneous nucleation is most favorable when the contact angle between the seed particle and the forming droplet is small. Heterogeneous nucleation probability depends strongly on the contact angle. Since the contact angle depends on the chemical composition of the vapour and the seed particle (equation 2.12), this is of special interest. In certain conditions, such as at a low enough vapour concentration and high enough saturation concentration, heterogeneous nucleation is improbable if the contact angle is large enough. For a uniform particle population where heterogeneous nucleation is ineffective, the rate of new particles forming will be higher compared to conditions where heterogeneous nucleation is more probable.

4.3.2 Dependency of Heterogeneous Nucleation on Vapour Concentration

Minimum contact angles needed for there to occur no heterogeneous nucleation were determined using the onset probability of 0.5 for different sulfuric acid concentrations and saturation concentrations. These contact angles will be referred as θ_{min} from hereon. In Figure 4.15 θ_{min} corresponding to different D_{seed} can be seen when the saturation concentration is $2.5 \times 10^5\,\mathrm{cm}^{-3}$ and the vapour concentration of sulfuric acid gets different values. The higher the vapour concentration, the higher the contact angle of nucleation needs to be for heterogeneous nucleation to be unfavorable. This is because the higher supersaturation means a lower energy of formation for a critical cluster as seen from equation 2.6.

Heterogeneous nucleation probabilities for sulfuric acid for different D_{seed} when $\theta = 90°$ are seen in Figure 4.16 assuming $c = 1 \times 10^7\,\mathrm{cm}^{-3}$ and $c_{sat} = 5 \times 10^5\,\mathrm{cm}^{-3}$. It is clear that for larger seed particles heterogeneous nucleation is more likely, which is due to both the dependency of geometric factor (equation 2.8) and nucleation probability (equation 2.17) on the size of the seed particle. For a larger seed, less surface has to be formed and collisions of vapour molecules with it are more likely. It can also be observed that the dependency of θ_{min} on the diameter of the seed particle D_{seed} gets stronger for higher vapour concentrations. Opposite behaviour can be noticed at the lower concentrations, where the contact angle seems to approach some constant with increasing seed diameter.

The vapour concentration was kept constant and the saturation concentration of the vapour was changed to investigate the dependency of heterogeneous nucleation

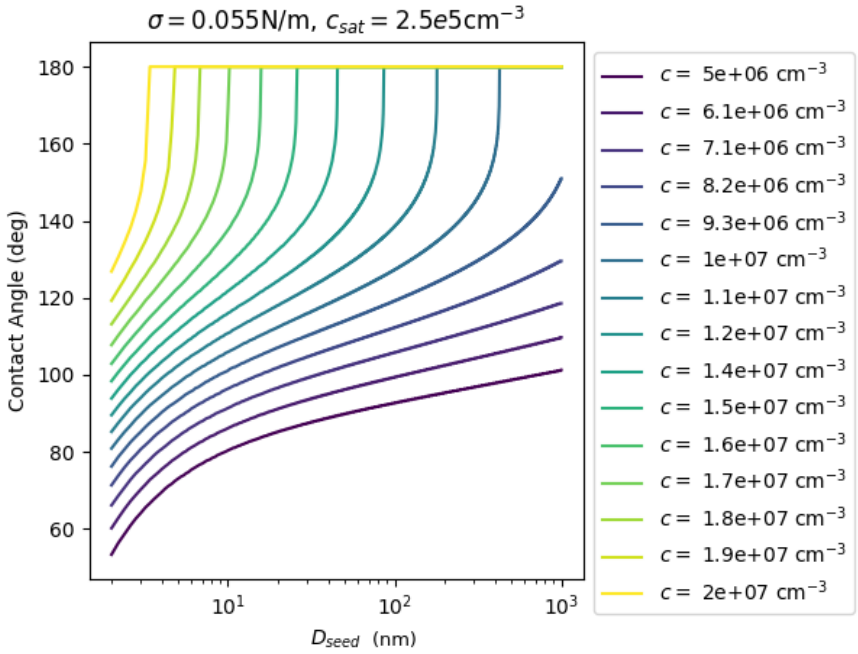

Figure 4.15: Contact Angles needed for no heterogeneous nucleation to occur for different diameter seed particles and vapour concentrations in the case of vapour similar to sulfuric acid (surface tension of 0.055 N/m)

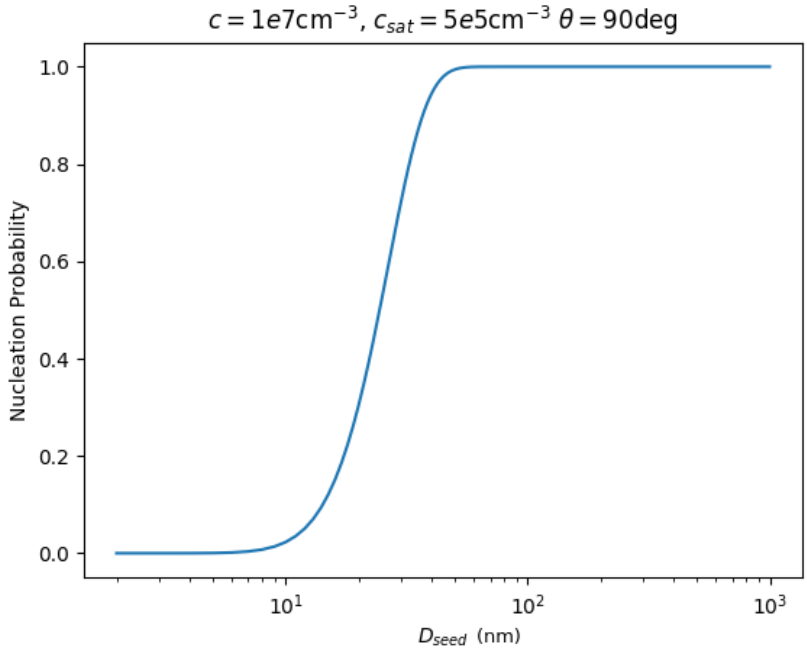

Figure 4.16: Dependency of nucleation probability on diameter of seed particle when sulfuric acid vapour concentration is $1 \times 10^7\,\mathrm{cm}^{-3}$, saturation concentration is $5 \times 10^5\,\mathrm{cm}^{-3}$ and contact angle is 90°.

probability on saturation concentration. The contact angles necessary for no nucleation for different saturation concentrations are shown in Figure 4.17. For higher saturation concentrations the saturation ratio is lower and more energy is needed for a critical cluster to be formed. Because of this a smaller contact angle is needed for there to be no nucleation if the saturation concentration is higher.

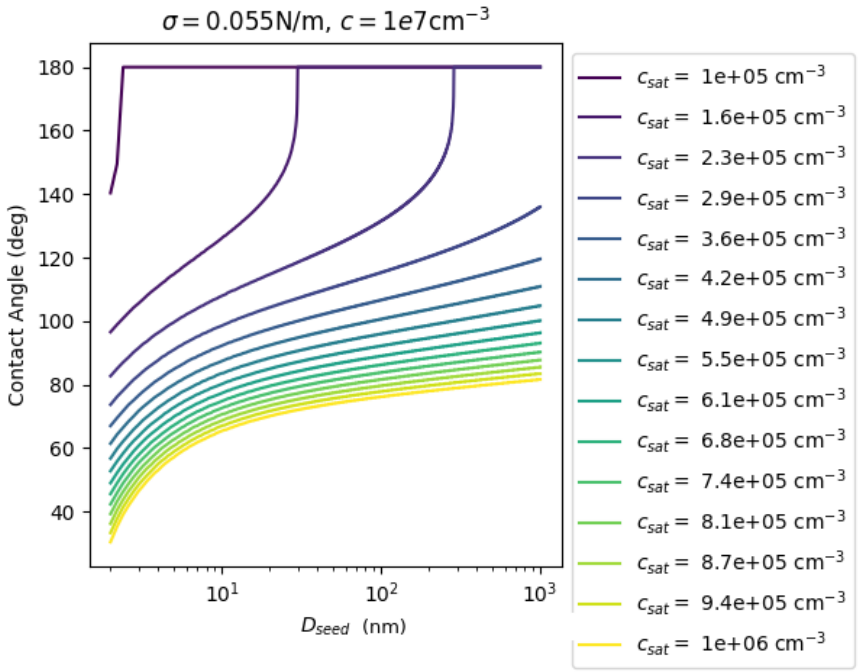

Figure 4.17: Contact Angles needed for no heterogeneous nucleation to occur for different diameters of seed particle and saturation concentrations for sulfuric acid.

Figure 4.18 shows the dependency of the free energy of formation of the critical radius on contact angle of heterogeneous nucleation. At a higher supersaturation, the formation energy is lower at all contact angles, illustrating that heterogeneous nucleation is more favorable. It can be also seen that the free energy dG_{het} approaches a maximum value with large contact angle and this value does not seem to depend on the size of the seed particle. In the cases of Figure 4.18, the nucleation probability only depends on the diameter of the particle through equation 2.17. In Figure 4.19 is shown the dependency of the free energy of formation for different vapour concentrations. The formation of critical radius takes more energy if the vapour concentration is lower. What is interesting is that for higher vapour concentrations, the difference between the energies needed to form a critical droplet is smaller for different contact angles, which favors heterogeneous nucleation even if the contact angle is large.

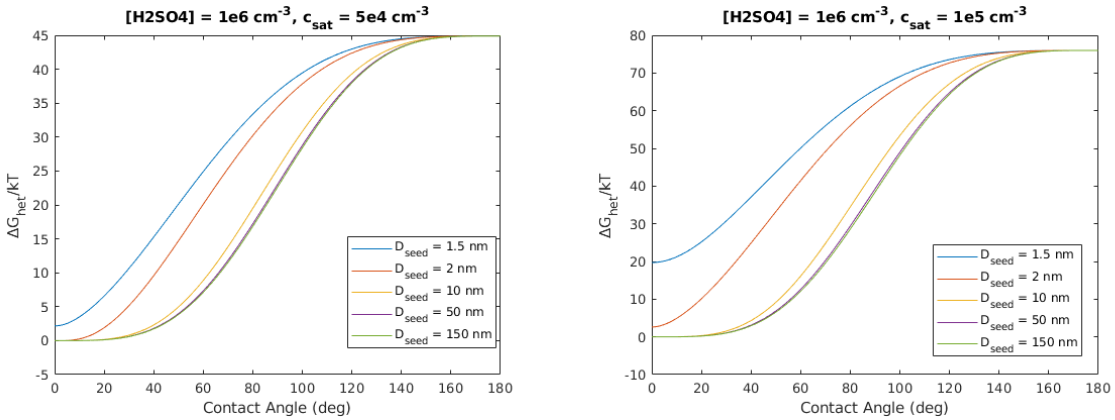

Figure 4.18: Formation free energy for different sized seed particles and contact angles when $c = 1 \times 10^6\,\mathrm{cm}^{-3}$ for sulfuric acid. In the left figure saturation concentration is $5 \times 10^4\,\mathrm{cm}^{-3}$ and in the right it is $1 \times 10^5\,\mathrm{cm}^{-3}$

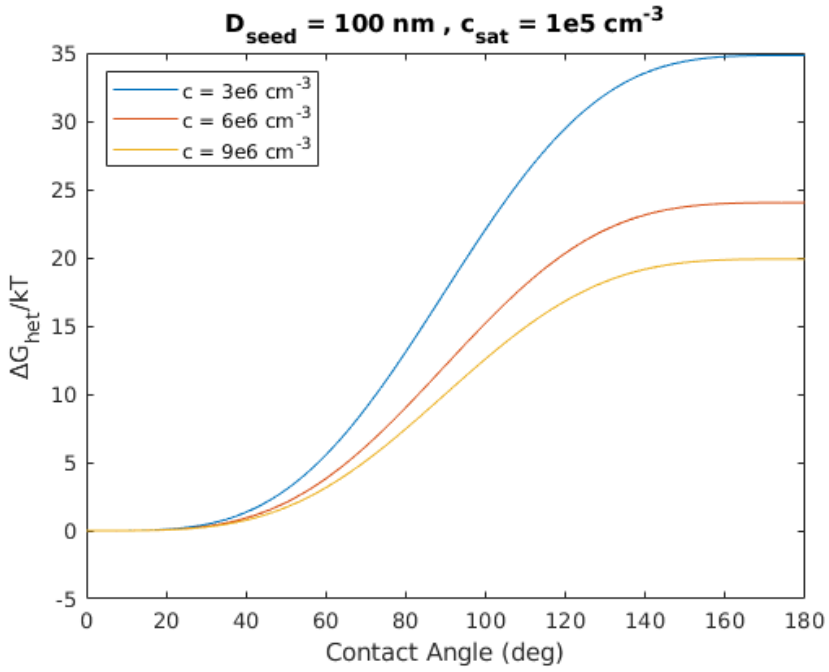

Figure 4.19: Formation free energy for different sulfuric acid vapour concentrations when seed diameter is 100 nm and saturation concentration is $1 \times 10^5\,\mathrm{cm}^{-3}$.

4.3.3 Dependency of Heterogeneous Nucleation on Surface Tension

Calculations were done with the mass and density corresponding to properties of sulfuric acid molecule but with different surface tensions varying from 0.02 N/m to 0.08 N/m. From Figures 4.20a and 4.20b, it can be seen that heterogeneous nucleation depends strongly on the surface tension of the vapour-liquid interface. Behaviour of contact angle as a function of seed diameter follows a similar pattern when either vapour con-

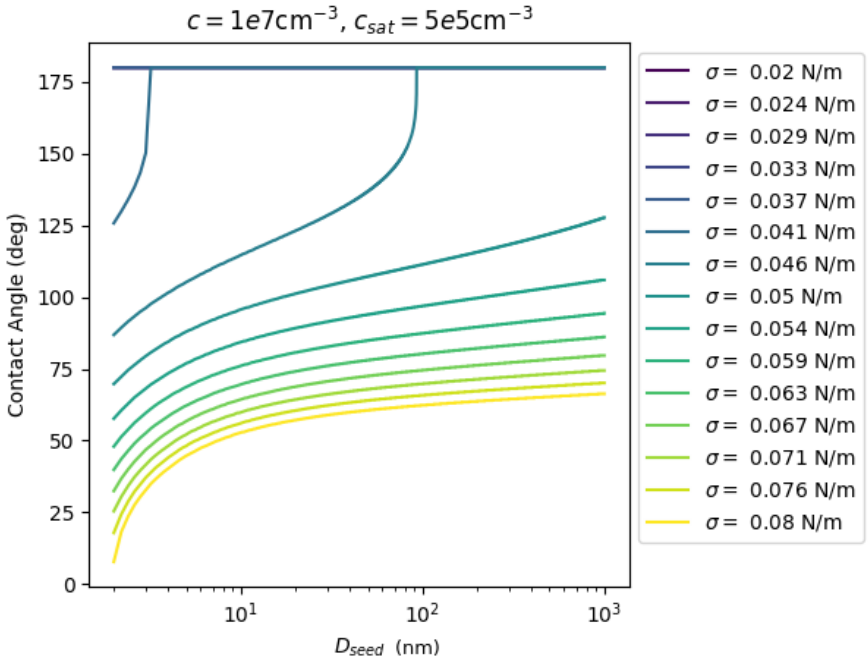

(a) Saturation concentration of $5 \times 10^5\,\mathrm{cm}^{-3}$.

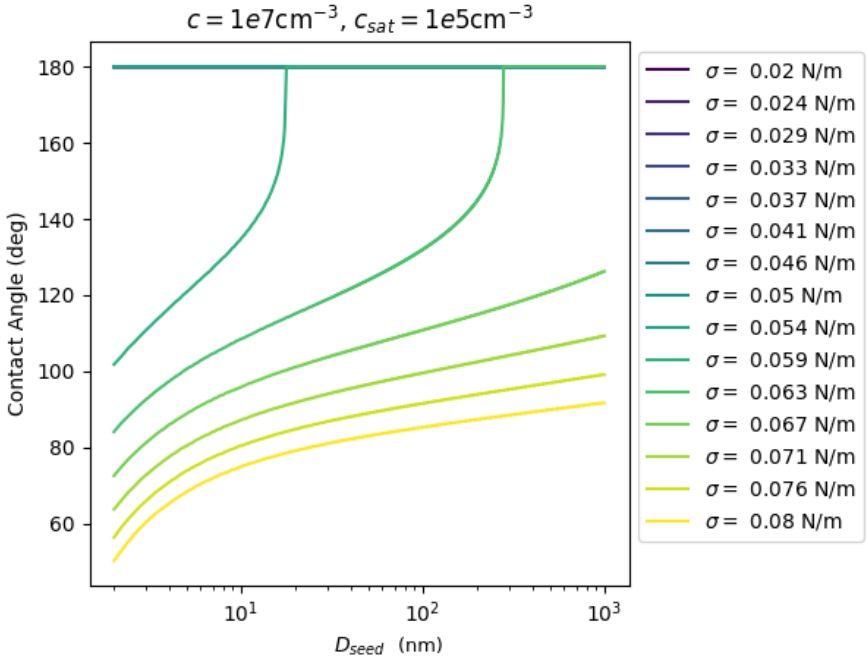

(b) Saturation concentration of $1 \times 10^5\,\mathrm{cm}^{-3}$

Figure 4.20: θ_{min} for different surface tensions and diameters of seed particle when vapour concentration is $1 \times 10^7\,\mathrm{cm}^{-3}$.

centration or saturation concentration is varied (for example Figure 4.17). Now with a higher surface tension, θ_{min} is smaller, which is because with a higher surface tension

the formation free energy of a critical cluster is also higher (equations 2.5 and 2.6). If $c = 1 \times 10^7\,\mathrm{cm}^{-3}$ and $c_{sat} = 5 \times 10^5\,\mathrm{cm}^{-3}$ for a seed diameter of 100 nm and surface tension of 0.05 N/m, the contact angle has to be over 110° for heterogeneous nucleation to be ineffective.

There is no heterogeneous nucleation when both the contact angle and surface tension are relatively high. It is less likely to find situations with no heterogeneous nucleation for a substance with low surface tension of liquid-gas interface compared to one with a higher surface tension. For example organics typically have rather small surface tensions [Korosi & Kovats, 1981]. However, organic molecules can also be rather large, which needs to be considered because mass of a vapour molecule also has an effect on nucleation probability.

4.3.4 Dependency of Heterogeneous Nucleation on Molecular Mass

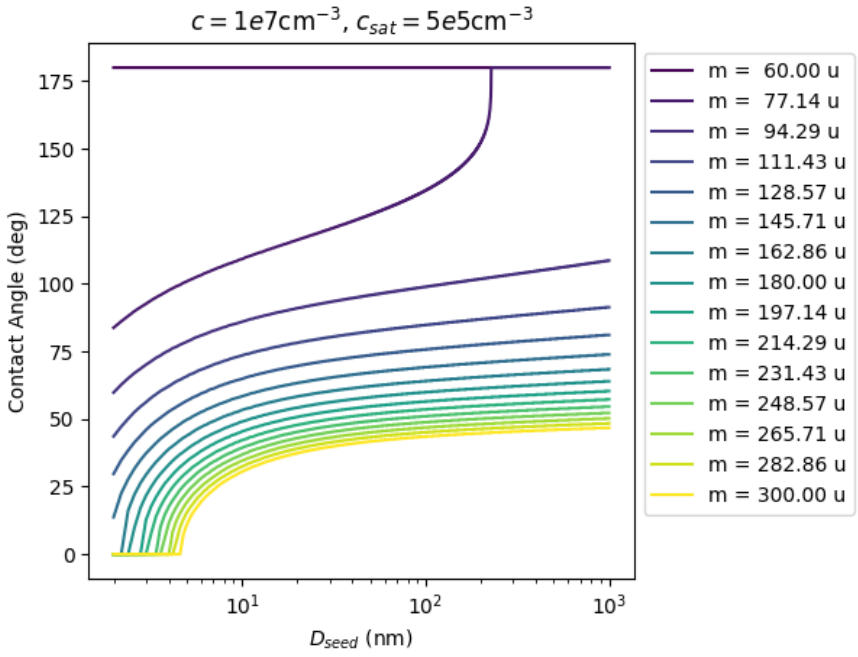

Figure 4.21: Contact angle needed for no nucleation for different molecular masses and diameters of seed particle in mass range 60 u - 300 u when vapour concentration is $1 \times 10^7\,\mathrm{cm}^{-3}$ and saturation concentration is $5 \times 10^5\,\mathrm{cm}^{-3}$.

Calculations were done with the surface tension and density of sulfuric acid but with different masses of vapour molecule in range 60 u - 600 u. As seen from Figure 4.21 θ_{min} is lower when the vapour molecules have larger mass and thus also larger volume. With a larger molecule, the critical radius is larger (equation 2.5) and more energy is

needed to form a critical cluster. When both nucleation contact angle and molecules are large, situations where there is no or little heterogeneous nucleation can exist. If sulfuric acid vapour concentration is $1 \times 10^7\,\mathrm{cm}^{-3}$ and saturation concentration $5 \times 10^5\,\mathrm{cm}^{-3}$ for a mass of 300 u a contact angle of below 50° is enough for heterogeneous nucleation to be ineffective even if the seed particle has a diameter of 1 µm.

Heterogeneous nucleation was calculated for even more massive vapour molecules than the ones presented in Figures 4.21 and 4.23. In Figure 4.22 there are θ_{min} for vapours of molecules with masses ranging from 500 u to 600 u. These could for example be masses of very massive organic molecules. If the seed particle has a diameter of 100 nm, even for a very massive molecule of 600 u heterogeneous nucleation will be probable unless the contact angle of nucleation is over 25°.

Figure 4.23 shows the dependency of the maximum contact angle for heterogeneous nucleation to occur on mass with the surface tension of 0.0275 N/m, which is half of the one used in Figures 4.21. This surface tension is closer to the surface tensions of many organic compounds. We can see that with a lower surface tension, which favors nucleation, the mass dependency is stronger. If the surface tension is low, the vapour molecule needs to have larger mass for there to not be any heterogeneous nucleation and smaller mass differences have a larger effect on the probability of heterogeneous nucleation.

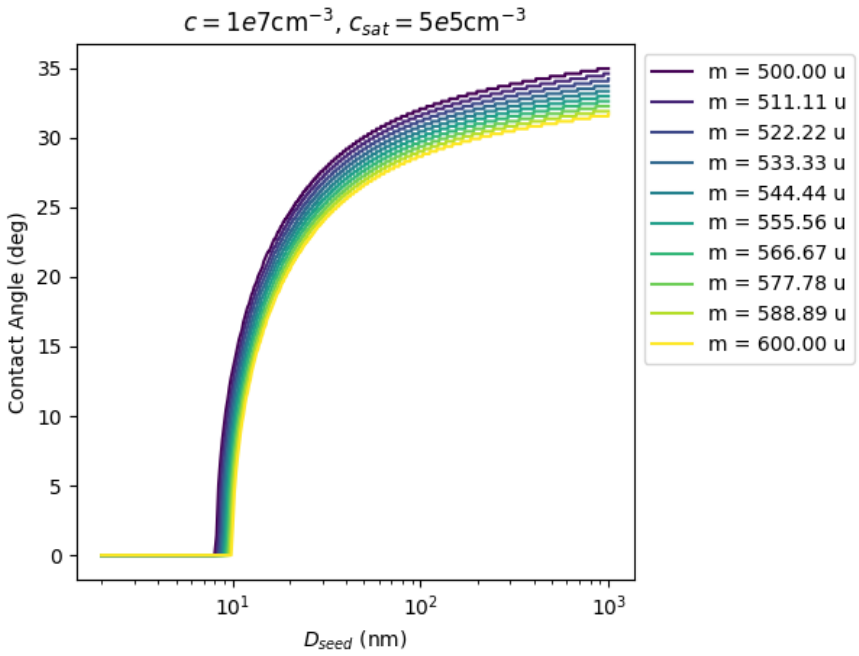

Figure 4.22: θ_{min} for different molecular masses and diameters of seed particle in mass range 500 u - 600 u when vapour concentration is $1 \times 10^7\,\mathrm{cm}^{-3}$ and saturation concentration is $5 \times 10^5\,\mathrm{cm}^{-3}$.

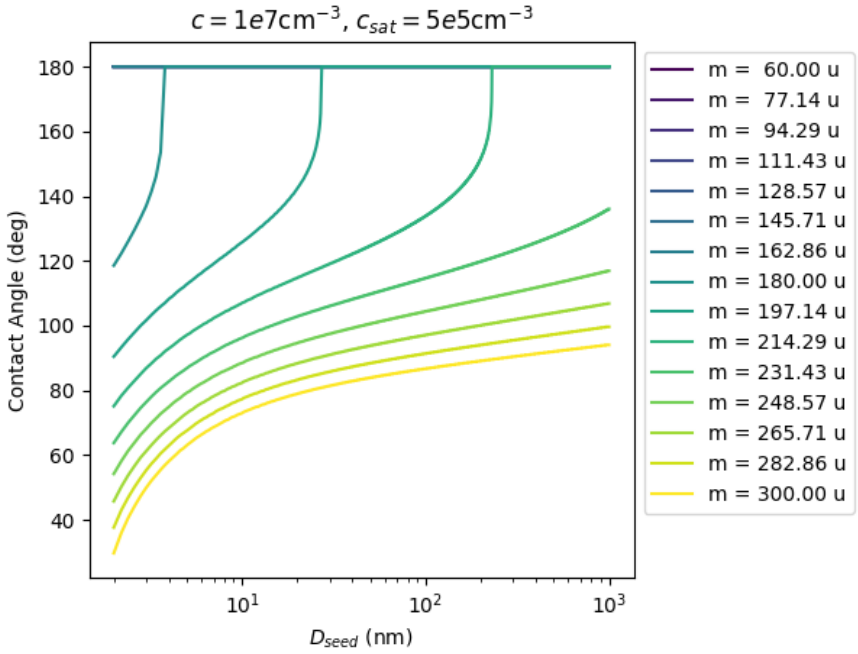

Figure 4.23: θ_{min} for different molecular masses and diameters of seed particle when surface tension is 0.0275 N/m in mass range 60 u - 300 u when vapour concentration is 1×10^7 cm^{-3} and saturation concentration is 5×10^5 cm^{-3}.

4.3.5 Heterogeneous Nucleation of Sulfuric Acid-DMA Clusters

Heterogeneous nucleation and the contact angles necessary for no nucleation were investigated for molecular clusters of sulfuric acid and DMA. Numbers of sulfuric acid and DMA molecules in the clusters varied from zero to four molecules. In a real situation the vapour would consist of clusters with different numbers of sulfuric acid and DMA molecules, but in this thesis it was approximated that the condensing vapour only has one type of clusters. Vapour concentration of 1×10^7 cm^{-3} was used and the saturation concentration was assumed to be 1×10^5 cm^{-3}, which means that the saturation ratio was 100 and the vapour was highly supersaturated.

Results are presented in Figures 4.24. Since DMA has a lower surface tension than sulfuric acid, for there to be no heterogeneous nucleation the contact angle has to be larger for pure DMA than for pure sulfuric acid. A cluster of N sulfuric acid molecules will also have a higher heterogeneous nucleation probability than a cluster with N sulfuric acid molecules with some DMA molecules since the latter will be heavier. In this case the effect a larger mass has is bigger that the effect of smaller surface tension because of the lower surface tension of dimethylamine compared to sulfuric acid.

From Figures 4.24c it can be seen that for a cluster of one sulfuric acid molecule

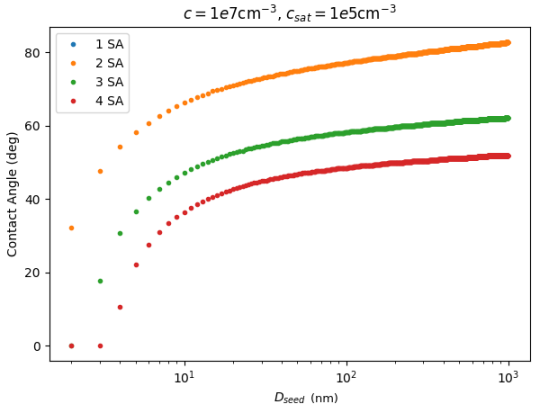

(a) θ_{min} for clusters of pure sulfuric acid.

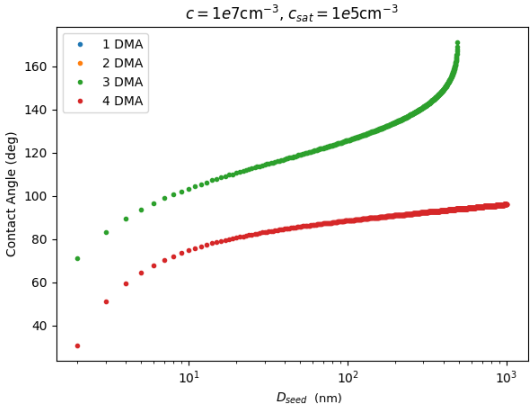

(b) θ_{min} for clusters of pure DMA.

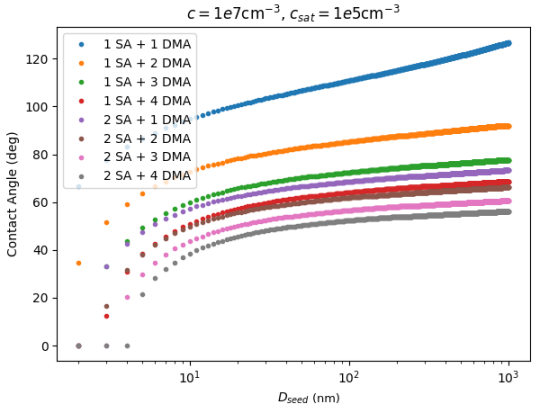

(c) θ_{min} for clusters with 1-2 sulfuric acid molecules

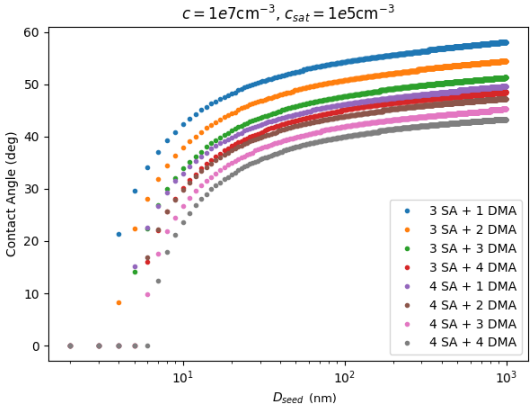

(d) θ_{min} for clusters with 3-4 sulfuric acid molecules

Figure 4.24: θ_{min} for clusters of sulfuric acid and dimethylamine.

and one DMA molecule, the contact angle of nucleation needs to be at least over 110° if the seed particle has a diameter of 100 nanometers for heterogeneous nucleation to be ineffective when vapour $c = 1 \times 10^7\,\mathrm{cm}^{-3}$ and $c_{sat} = 1 \times 10^5\,\mathrm{cm}^{-3}$. In such a situation no clusters with both sulfuric acid and DMA would condense on any particles with diameters below 100 nm. If there are two sulfuric acid and two DMA molecules a smaller contact angle of 60° will be sufficient. Taking into account the fact that for sulfuric acid on sulfur the contact angle is about 70° [Hamill et al., 1982] it seems completely possible for contact angle to be over 60°. It is also noteworthy that even for vapour of clusters of 4 sulfuric acid and 4 DMA molecules the contact angle needs to be over 30° for there to be no nucleation on a seed particle with a diameter of 100 nm.

If the vapour concentration is twofold compared to the one used in Figures 4.24, the contact angles needed for nucleation to be unfavorable will naturally be higher. It can be seen from Figure 4.25 that for a cluster with four sulfuric acid and two DMA molecules with vapour concentration of $2 \times 10^7\,\mathrm{cm}^{-3}$, the contact angle needs to close

to 50° for there to be no nucleation on a 100 nm seed. This is about 10° more than for the smaller vapour concentration of $1 \times 10^7\,\mathrm{cm}^{-3}$. For clusters with one sulfuric acid and one DMA molecule for a 100 nm diameter seed, there will now always be heterogeneous nucleation unless the seed particle material completely repels the condensing compound, compared to the situation before where there would be no heterogeneous nucleation for angles over 110° (Figure 4.24c). For the vapour consisting of smaller clusters and with a smaller surface tension of liquid-vapour interface, properties that favour heterogeneous nucleation, the difference caused in value of θ_{min} caused by a larger vapour concentration is also larger.

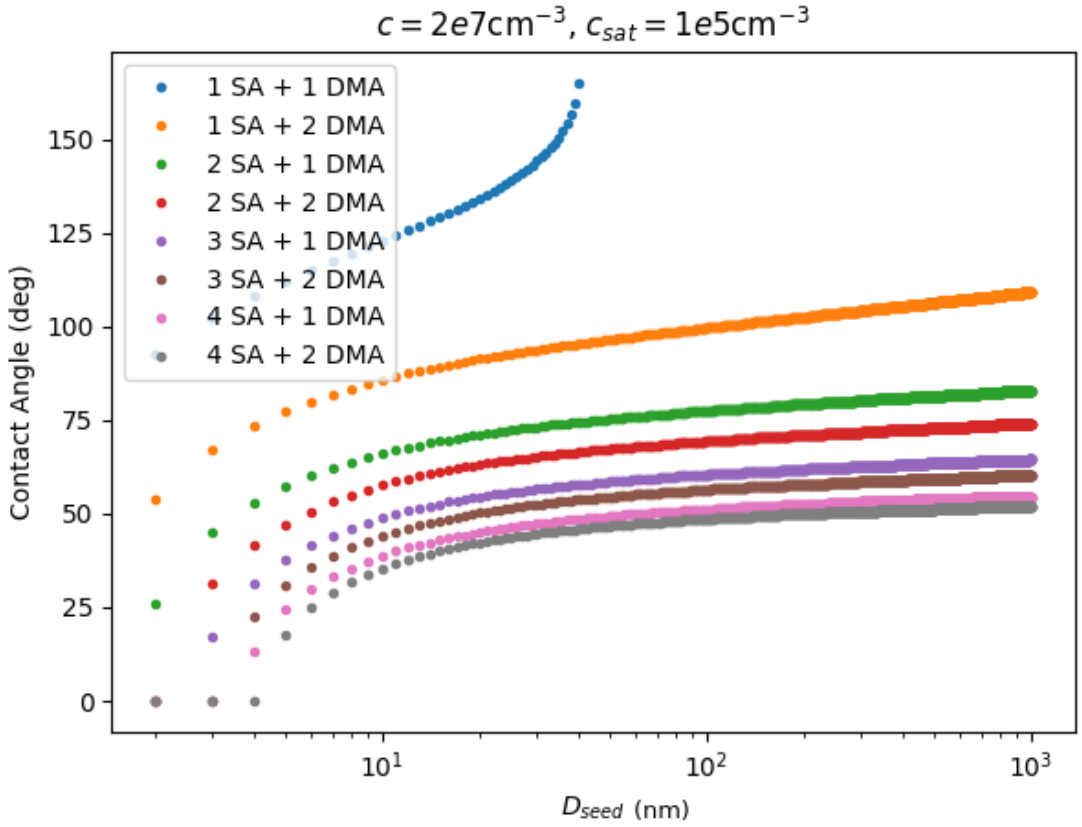

Figure 4.25: Maximum contact angles for nucleation to occur for clusters of sulfuric acid and dimethylamine with vapour concentration of $2 \times 10^7\,\mathrm{cm}^{-3}$

4.3.6 Heterogeneous Nucleation of LVOC

Heterogeneous nucleation of low-volatile organic compounds was considered for different sized clusters consisting of an exemplary LVOC molecule. Its mass is approximately 203 u and its surface tension is 0.02 N/m. All the properties of the exemplary molecule can be found in Table 3.5. The minimum contact angles θ_{min} required for LVOC clusters to not effectively partake in heterogeneous nucleation are in Figures 4.26. We can

see from Figure 4.26a that for vapour of single LVOC molecules heterogeneous nucleation will occur no matter the contact angle when vapour concentration is $1 \times 10^8\,\mathrm{cm}^{-3}$. This is mainly due to the low surface tension of low-volatile organic compounds. For a cluster of two model molecules a large contact angle of little over 100° will be enough for no heterogeneous nucleation to happen when the seed particle has a diameter of 100 nm. For a very massive cluster of 6 model LVOC molecules an angle of around 40° is enough even if the seed particle has a diameter close to 1 µm. Very large organic molecules are unlikely to partake in heterogeneous nucleation if the contact angle is not smaller than that.

With a vapour concentration of $2 \times 10^8\,\mathrm{cm}^{-3}$, θ_{min} gets larger values as seen from Figure 4.26b. Now if the seed particle has a diameter of 100 nm and the vapour consist of clusters of two LVOC there will be heterogeneous nucleation even for very large contact angles. However, for a massive cluster of 6 LVOC, a contact angle of above 40° is enough for heterogeneous nucleation to be inefficient. This is close to the corresponding value when $c = 1 \times 10^8\,\mathrm{cm}^{-3}$.

As shown in Figure 4.26c, if LVOC vapour concentration is $5 \times 10^7\,\mathrm{cm}^{-3}$ there still does not exists situations where heterogeneous nucleation is ineffective for single molecules similarly to if $c = 1 \times 10^8\,\mathrm{cm}^{-3}$ or $c = 2 \times 10^8\,\mathrm{cm}^{-3}$. However, for clusters of two LVOC molecules a contact angle of a bit above 80° is enough for heterogeneous nucleation to be ineffective when diameter of seed particle is 100 nm.

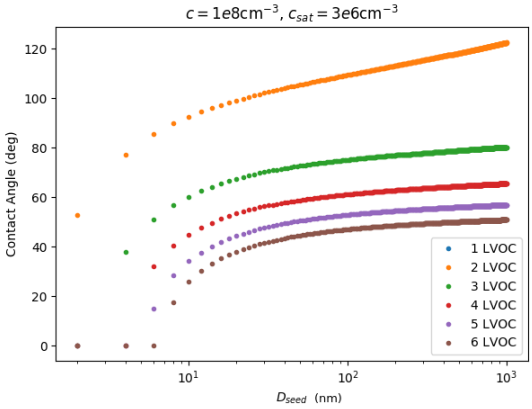

(a) Vapour concentration of $1 \times 10^8\,\mathrm{cm}^{-3}$

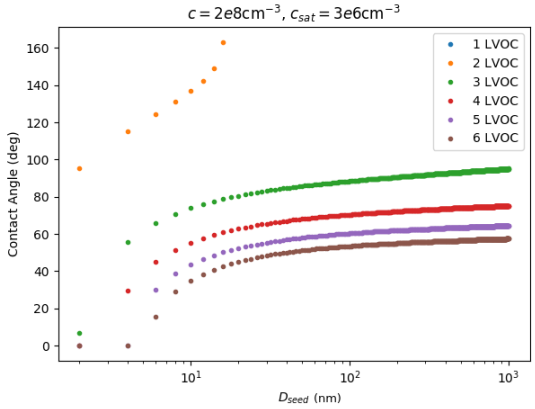

(b) Vapour concentration of $2 \times 10^8\,\mathrm{cm}^{-3}$

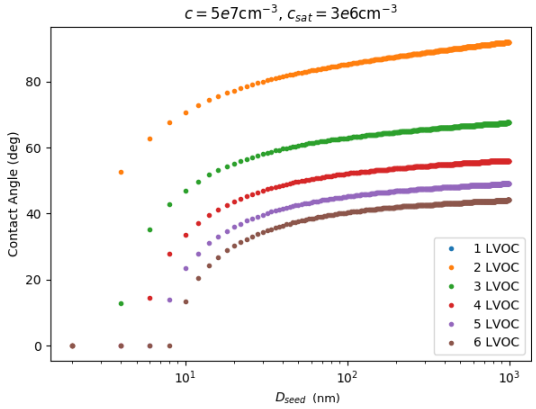

(c) Vapour concentration of $5 \times 10^7\,\mathrm{cm}^{-3}$

Figure 4.26: Maximum contact angles for nucleation to occur for clusters of LVOC molecule

4.4 Condensation Sink and Heterogeneous Nucleation

Calculated ratios of condensation sink and effective condensation sink for different minimum diameters (Figure 3.2) were used alongside with the heterogeneous nucleation results so that the diameters corresponding to values of θ_{min} were assumed to be equivalent to the minimum diameters. This in practice means that in a particle population all particles under a certain size would not participate in the condensation sink of certain vapour molecules or clusters because for them the contact angle of nucleation is too high for heterogeneous nucleation to occur. In a system with growing particles particles cannot function as seed particles until they have grown to a certain size by other means than heterogeneous nucleation. These assumptions are only valid if for most of the particle population the contact angle of heterogeneous nucleation of the vapour would be similar meaning that they are close in chemical composition.

The values of CS_{eff}/CS and the corresponding minimum diameters are shown in Figure 3.2 and the median number size distribution used is shown in Figure 3.1.

Figure 4.27 shows the ratios of effective condensation sink and the actual condensation sink for different conditions such as vapour concentrations between $5 \times 10^6\,\mathrm{cm}^{-3}$ and $2 \times 10^7\,\mathrm{cm}^{-3}$, saturation concentration between $1 \times 10^5\,\mathrm{cm}^{-3}$ and $1 \times 10^6\,\mathrm{cm}^{-3}$, vapour molecule mass between 60 u and 300 u and surface tension between 0.02 N/m and 0.08 N/m , versus the corresponding contact angle that is the minimum required for heterogeneous nucleation to be ineffective.

It can be seen that for most situations the contact angle has to be considerably large to have a significant effect on the condensation sink. For example for sulfuric acid on sulfur the contact angle is around 70° [Hamill et al., 1982] and assuming a saturation concentration of $5 \times 10^5\,\mathrm{cm}^{-3}$ there would be barely any effect on the condensation sink in the range of studied concentrations according to Figure 4.27a. If the contact angle is 75° and the vapour concentration $5 \times 10^6\,\mathrm{cm}^{-3}$, sulfuric acid would have an effective condensation sink that would be about 20% of the actual condensation sink when $c_{sat} = 5 \times 10^5\,\mathrm{cm}^{-3}$.

If vapour concentration is $1 \times 10^7\,\mathrm{cm}^{-3}$ the effect a nucleation contact angle has on condensation sink of sulfuric acid for different saturation concentrations are shown in Figure 4.27b. If the saturation concentration is $1 \times 10^5\,\mathrm{cm}^{-3}$ there is no effect on the condensation sink of sulfuric acid unless sulfuric acid and the seed particle completely repel each other ($\theta = 180°$).

Assuming the vapour molecule has otherwise the properties of sulfuric acid but its surface tension is 0.08 N/m, when vapour concentration is $1 \times 10^7\,\mathrm{cm}^{-3}$, saturation concentration is $5 \times 10^5\,\mathrm{cm}^{-3}$ and the contact angle is 70° the effective condensation for the vapour is practically zero as shown in Figure 4.27b. However, if the surface tension is 0.041 N/m or lower, there is no effect on condensation sink unless the seed and vapour completely repel each other.

If the vapour molecule has otherwise the same properties of sulfuric acid but its mass is 300 u, assuming a vapour concentration of $1 \times 10^7\,\mathrm{cm}^{-3}$ and saturation concentration of $5 \times 10^5\,\mathrm{cm}^{-3}$, the contact angle only has to be somewhere around 40° for effective condensation sink to be half of the condensation sink as shown in Figure 4.27d. If the mass is instead 200 u, the contact angle has to be around 60° to have the same effect on condensation of the vapour.

If the nucleating vapour consists of sulfuric acid and DMA clusters, assuming a contact angle of nucleation for a particle population, the effects the contact angle would have on the condensation sink of these clusters are shown in Figures 4.28, when vapour concentration is $1 \times 10^7\,\mathrm{cm}^{-3}$ and saturation concentration is $1 \times 10^5\,\mathrm{cm}^{-3}$. If the cluster has one sulfuric acid and one DMA molecule, the contact angle has to be

over 100° to have an effect on the condensation sink and over 110° for the effective condensation sink to be 50 % of condensation sink or smaller.

For a cluster of three sulfuric acid molecules and one DMA molecule, it would be enough if the contact angle would be about 60° for the effective condensation sink of the seed particle population to be close to zero. In the atmosphere, a real nucleating vapour would consist of clusters with different numbers of sulfuric acid and DMA and if the average contact angle would be about 60°, all clusters with at least three sulfuric acid molecules and one DMA would not take part in heterogeneous nucleation. They would not stick in the event of a collision with a particle.

Clusters of LVOC molecules were similarly considered. It can be seen from Figure 4.29 that for vapour of clusters of two molecules, the contact angle for the seed population has to be over 110° to have a significant effect on the condensation sink. For clusters of six model LVOC molecules, contact angle of above 45° is enough to make a difference of 50 % to their condensation sink. However if a cluster consists of just a single LVOC molecule, there will be no effect on its condensation sink unless it is completely repelled by seed particles.

As mentioned before in this thesis, new particle formation events are detected in very polluted conditions in China. Because of the very large condensation sink, this should be theoretically impossible. However, as shown here, multiple factors such as a large contact angle of heterogeneous nucleation or large molecular mass can cause the condensation sink to be significantly lower than theory theoretically predicted. This results in significantly different conditions where new particle formation and probability of new particle formation events occurring has to be reconsidered.

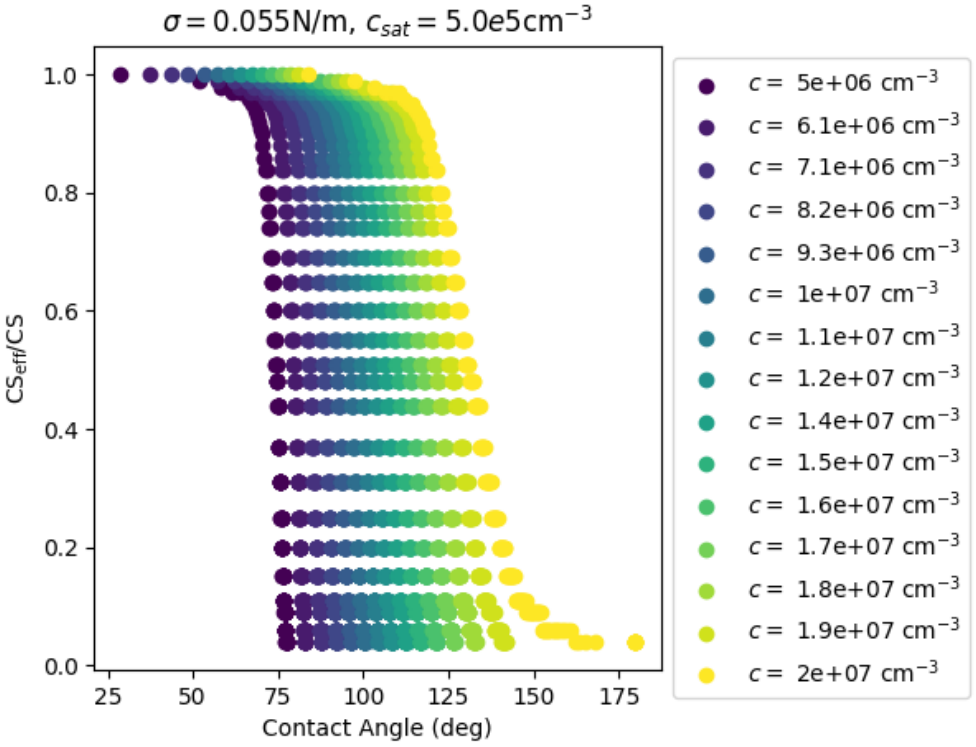

(a) Concentration of sulfuric acid vapour is between $5 \times 10^6\,\mathrm{cm}^{-3}$ and $2 \times 10^7\,\mathrm{cm}^{-3}$ and saturation concentration is $5 \times 10^5\,\mathrm{cm}^{-3}$

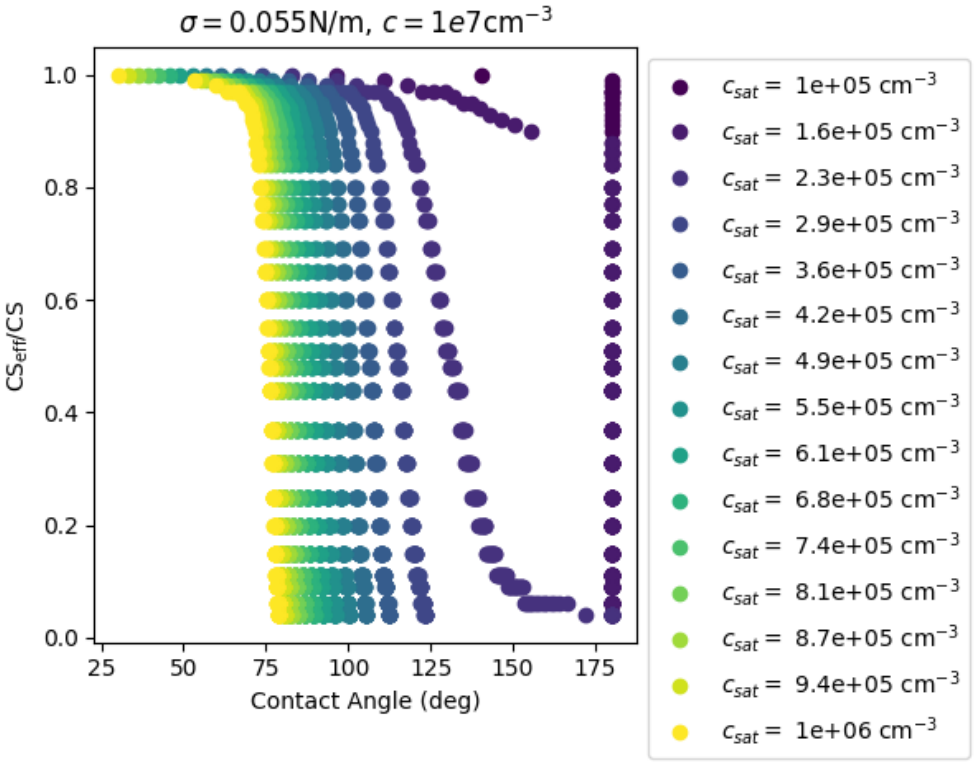

(b) Concentration of sulfuric acid vapour is $1 \times 10^7\,\mathrm{cm}^{-3}$ and vapour concentration is between $1 \times 10^5\,\mathrm{cm}^{-3}$ and $1 \times 10^6\,\mathrm{cm}^{-3}$

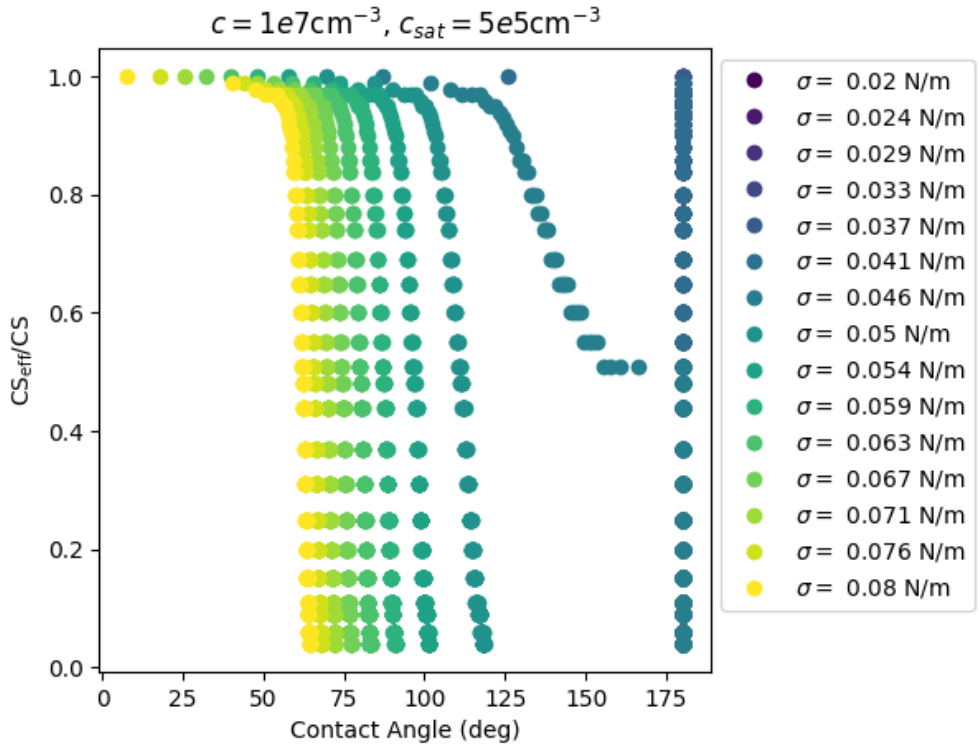

(c) Vapour concentration is $1 \times 10^7\,\text{cm}^{-3}$ and saturation concentration is $5 \times 10^5\,\text{cm}^{-3}$. Surface tension is between $0.02\,\text{N/m}$ and $0.08\,\text{N/m}$

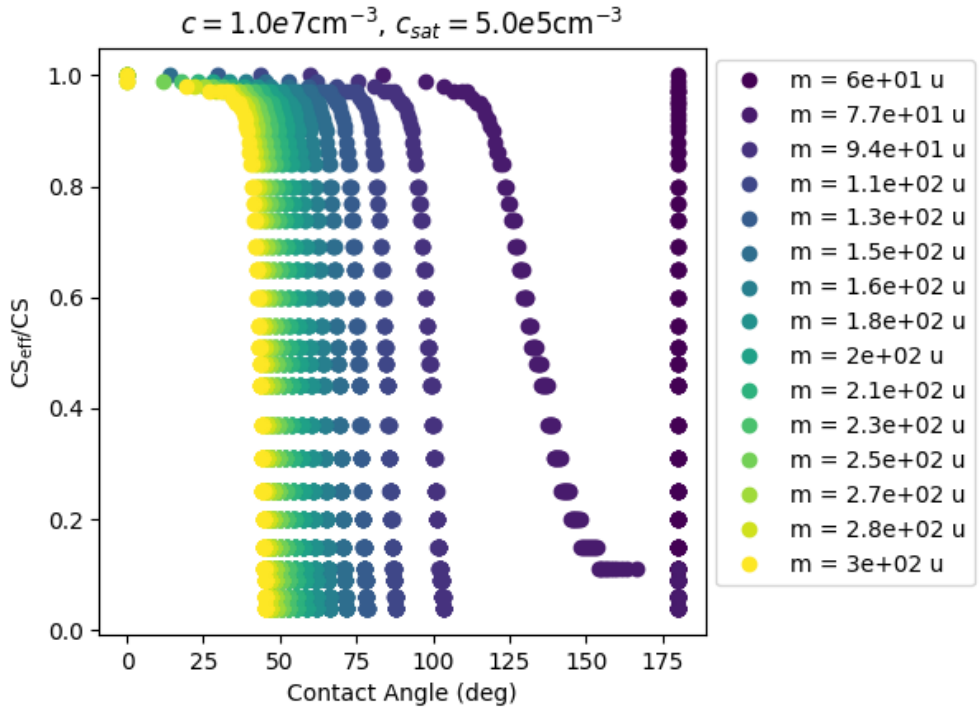

(d) Vapour concentration is $1 \times 10^7\,\text{cm}^{-3}$ and saturation concentration is $5 \times 10^5\,\text{cm}^{-3}$. Vapour molecule mass is between $60\,\text{u}$ and $300\,\text{u}$

Figure 4.27: Ratio of effective condensation sink and condensation sink $\text{CS}_{\text{eff}}/\text{CS}$ as a function of θ_{min} in different conditions.

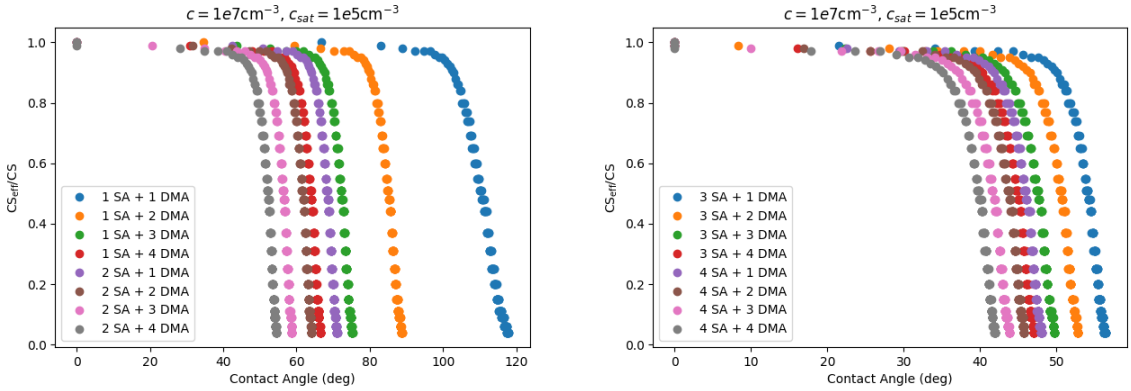

Figure 4.28: θ_{min} for clusters of sulfuric acid and dimethylamine and the corresponding CS_{eff}/CS

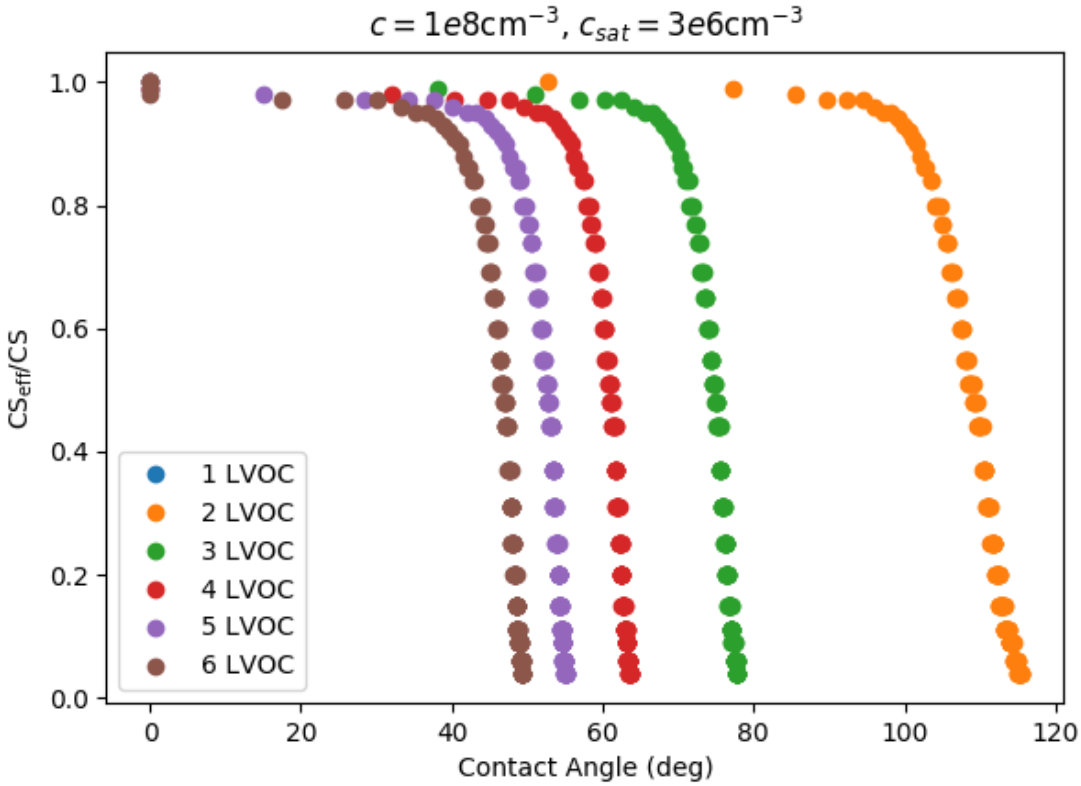

Figure 4.29: θ_{min} for clusters of a model LVOC molecule and the corresponding CS_{eff}/CS

5. Conclusions

The purpose of this thesis was to explore possible explanations for why there are frequent observations of New Particle Formation Events in China despite heavy pollution and resulting high condensation sink. Reasons for effective condensation sink to be smaller than the measured condensation sink were studied and the influences of aerosol chemical composition and ineffective heterogeneous nucleation on effective condensation sink were considered.

In this thesis heterogeneous nucleation probabilities were studied based on Classical Nucleation Theory. Vapours consisting of clusters of sulfuric acid and dimethylamine and clusters of LVOC molecules were considered. The dependency of heterogeneous nucleation probability on different variables such as surface tension and molecular mass was also investigated by changing the properties of the vapour. Special attention was given to the contact angle of heterogeneous nucleation and how it affects the likelihood of nucleation. Because contact angle depends on the surface tensions of the condensing vapour and the condensing surface, the effect of aerosol chemical composition measured in Beijing on the ratio of survival probability and survival parameter was also investigated. This could have given implications about the dependency of effective condensation sink on the chemical composition of aerosol.

Multiple approximations and simplifications were done in heterogeneous nucleation calculations in this thesis. Some approximations were made about the values and variables used in the heterogeneous nucleation model. All calculations were also done assuming unary nucleation. All of this was done to simplify the model while still trying to give valid indications of heterogeneous nucleation in different atmospheric conditions and for different nucleating vapours.

The probability of heterogeneous nucleation was found to be very strongly dependent on the contact angle of heterogeneous nucleation, surface tension of the liquid-vapour interface of the condensing droplet and the mass of the vapour monomers. It was found that larger the contact angle or molecular mass the smaller the heterogeneous nucleation probability is. A lower surface tension however resulted in a higher probability of nucleation. If heterogeneous nucleation is ineffective for certain molecules or clusters, they are not affected by a condensation sink caused by particle population

to the same extent as others. This could cause a significantly smaller effective condensation sink compared to the theoretical condensation sink, explaining at least in part why new particle formation events are detected in heavily polluted environments in China.

The contact angle of heterogeneous nucleation is affected by chemical composition of the condensation surface such as a seed particle. Aerosol chemical composition was analyzed alongside with formation rates, condensation sink and growth rates, which was done based on measurement data. However, no clear indications on a possible connection between chemical composition and effective condensation sink was found in this thesis. More detailed analysis of measurement data is needed to be able to answer whether aerosol chemical composition and effective condensation sink are connected.

The purpose of this thesis was to study behaviour of heterogeneous nucleation probability and explore the possible connection between effective condensation sink and ineffective heterogeneous nucleation and whether this could explain observed new particle formation in heavily polluted conditions. These objectives were fulfilled and this thesis does its part in deepening our understanding of heterogeneous nucleation and effective condensation sink.

Bibliography

[Asmi et al., 2010] Asmi, E., Frey, A., Virkkula, A., Ehn, M., Manninen, H., Timonen, H., Tolonen-Kivimäki, O., Aurela, M., Hillamo, R., & Kulmala, M. (2010). Hygroscopicity and chemical composition of antarctic sub-micrometre aerosol particles and observations of new particle formation. *Atmospheric Chemistry and physics*, 10(9), 4253–4271.

[Butt et al., 2003] Butt, H.-J., Butt, H.-J. B., Graf, K., & Kappl, M. (2003). *Physics and chemistry of interfaces*. John Wiley & Sons.

[Ehn et al., 2014] Ehn, M., Thornton, J. A., Kleist, E., Sipilä, M., Junninen, H., Pullinen, I., Springer, M., Rubach, F., Tillmann, R., Lee, B., et al. (2014). A large source of low-volatility secondary organic aerosol. *Nature*, 506(7489), 476.

[Fletcher, 1958] Fletcher, N. (1958). Size effect in heterogeneous nucleation. *The Journal of chemical physics*, 29(3), 572–576.

[Franck et al., 2011] Franck, U., Odeh, S., Wiedensohler, A., Wehner, B., & Herbarth, O. (2011). The effect of particle size on cardiovascular disorders — the smaller the worse. *Science of The Total Environment*, 409(20), 4217 – 4221.

[Hamill et al., 1982] Hamill, P., Turco, R., Kiang, C., Toon, O., & Whitten, R. (1982). An analysis of various nucleation mechanisms for sulfate particles in the stratosphere. *Journal of Aerosol Science*, 13(6), 561–585.

[Haynes, 2014] Haynes, W. M. (2014). *CRC handbook of chemistry and physics*. CRC press.

[Kerminen et al., 2018] Kerminen, V.-M., Chen, X., Vakkari, V., Petäjä, T., Kulmala, M., & Bianchi, F. (2018). Atmospheric new particle formation and growth: review of field observations. *Environmental Research Letters*, 13(10), 103003.

[Kerminen & Kulmala, 2002] Kerminen, V.-M. & Kulmala, M. (2002). Analytical formulae connecting the “real” and the “apparent” nucleation rate and the nuclei num-

ber concentration for atmospheric nucleation events. *Journal of Aerosol Science*, 33(4), 609–622.

[Kim et al., 2015] Kim, K.-H., Kabir, E., & Kabir, S. (2015). A review on the human health impact of airborne particulate matter. *Environment international*, 74, 136–143.

[Kirkby et al., 2011] Kirkby, J., Curtius, J., Almeida, J., Dunne, E., Duplissy, J., Ehrhart, S., Franchin, A., Gagne, S., Ickes, L., Kuerten, A., Kupc, A., Metzger, A., Riccobono, F., Rondo, L., Schobesberger, S., Tsagkogeorgas, G., Wimmer, D., Amorim, A., Bianchi, F., Breitenlechner, M., David, A., Dommen, J., Downard, A., Ehn, M., Flagan, R. C., Haider, S., Hansel, A., Hauser, D., Jud, W., Junninen, H., Kreissl, F., Kvashin, A., Laaksonen, A., Lehtipalo, K., Lima, J., Lovejoy, E. R., Makhmutov, V., Mathot, S., Mikkila, J., Minginette, P., Mogo, S., Nieminen, T., Onnela, A., Pereira, P., Petaja, T., Schnitzhofer, R., Seinfeld, J. H., Sipila, M., Stozhkov, Y., Stratmann, F., Tome, A., Vanhanen, J., Viisanen, Y., Vrtala, A., Wagner, P. E., Walther, H., Weingartner, E., Wex, H., Winkler, P. M., Carslaw, K. S., Worsnop, D. R., Baltensperger, U., & Kulmala, M. (2011). Role of sulphuric acid, ammonia and galactic cosmic rays in atmospheric aerosol nucleation. *NATURE*, 476(7361), 429–U77.

[Koponen et al., 2003] Koponen, I. K., Virkkula, A., Hillamo, R., Kerminen, V.-M., & Kulmala, M. (2003). Number size distributions and concentrations of the continental summer aerosols in queen maud land, antarctica. *Journal of Geophysical Research: Atmospheres*, 108(D18).

[Korosi & Kovats, 1981] Korosi, G. & Kovats, E. S. (1981). Density and surface tension of 83 organic liquids. *Journal of Chemical and Engineering Data*, 26(3), 323–332.

[Kulmala & Kerminen, 2008] Kulmala, M. & Kerminen, V.-M. (2008). On the formation and growth of atmospheric nanoparticles. *Atmospheric Research*, 90(2), 132 – 150. 17th International Conference on Nucleation and Atmospheric Aerosols.

[Kulmala et al., 2004a] Kulmala, M., Kerminen, V.-M., Anttila, T., Laaksonen, A., & O'Dowd, C. D. (2004a). Organic aerosol formation via sulphate cluster activation. *Journal of Geophysical Research: Atmospheres*, 109(D4).

[Kulmala et al., 2017] Kulmala, M., Kerminen, V.-M., Petäjä, T., Ding, A., & Wang, L. (2017). Atmospheric gas-to-particle conversion: why npf events are observed in megacities? *Faraday discussions*, 200, 271–288.

[Kulmala et al., 2014] Kulmala, M., Petäjä, T., Ehn, M., Thornton, J., Sipilä, M., Worsnop, D., & Kerminen, V.-M. (2014). Chemistry of atmospheric nucleation: on the recent advances on precursor characterization and atmospheric cluster composition in connection with atmospheric new particle formation. *Annual review of physical chemistry*, 65, 21–37.

[Kulmala et al., 2012] Kulmala, M., Petäjä, T., Nieminen, T., Sipilä, M., Manninen, H. E., Lehtipalo, K., Dal Maso, M., Aalto, P. P., Junninen, H., Paasonen, P., et al. (2012). Measurement of the nucleation of atmospheric aerosol particles. *Nature protocols*, 7(9), 1651.

[Kulmala et al., 2004b] Kulmala, M., VehkamÃ¤ki, H., PetÃ¤jÃ¤, T., Maso, M. D., Lauri, A., Kerminen, V.-M., Birmili, W., & McMurry, P. (2004b). Formation and growth rates of ultrafine atmospheric particles: a review of observations. *Journal of Aerosol Science*, 35(2), 143 – 176.

[Laden et al., 2000] Laden, F., Neas, L. M., Dockery, D. W., & Schwartz, J. (2000). Association of fine particulate matter from different sources with daily mortality in six us cities. *Environmental health perspectives*, 108(10), 941–947.

[Lauri, 2006] Lauri, A. (2006). Theoretical and computational approaches on heterogenous nucleation.

[Lazaridis, 1991] Lazaridis, M. (1991). Heterogenous nucleation.

[Lazaridis et al., 1992] Lazaridis, M., Kulmala, M., & Gorbunov, B. Z. (1992). Binary heterogeneous nucleation at a non-uniform surface. *Journal of aerosol science*, 23(5), 457–466.

[Lazaridis et al., 1991] Lazaridis, M., Kulmala, M., & Laaksonen, A. (1991). Binary heterogeneous nucleation of a water-sulphuric acid system: The effect of hydrate interaction. *Journal of aerosol science*, 22(7), 823–830.

[Lehtinen et al., 2007] Lehtinen, K. E., Maso, M. D., Kulmala, M., & Kerminen, V.-M. (2007). Estimating nucleation rates from apparent particle formation rates and vice versa: Revised formulation of the kerminenâ€“kulmala equation. *Journal of Aerosol Science*, 38(9), 988 – 994.

[Lehtipalo et al., 2016] Lehtipalo, K., Rondo, L., Kontkanen, J., Schobesberger, S., Jokinen, T., Sarnela, N., Kürten, A., Ehrhart, S., Franchin, A., Nieminen, T., Riccobono, F., Sipilä, M., Yli-juuti, T., Duplissy, J., Adamov, A., Ahlm, L., Almeida, J., Amorim, A., Bianchi, F., Breitenlechner, M., Dommen, J., Downard, A. J., Dunne,

E. M., Flagan, R. C., Guida, R., Hakala, J., Hansel, A., Jud, W., Kangasluoma, J., Kerminen, V.-m., Keskinen, H., Kim, J., Kirkby, J., Kupc, A., Kupiainen-määttä, O., Laaksonen, A., Lawler, M. J., Leiminger, M., Mathot, S., Olenius, T., Ortega, I. K., Onnela, A., Petäjä, T., Praplan, A., Rissanen, M. P., Ruuskanen, T., Santos, F. D., Schallhart, S., Schnitzhofer, R., Simon, M., Smith, J. N., Tröstl, J., Tsagkogeorgas, G., Tomé, A., Vaattovaara, P., Vehkamäki, H., Vrtala, A. E., Wagner, P. E., Williamson, C., Wimmer, D., Winkler, P. M., Virtanen, A., Donahue, N. M., Carslaw, K. S., Baltensperger, U., Riipinen, I., Curtius, J., Worsnop, D. R., & Kulmala, M. (2016). The effect of acid-base clustering and ions on the growth of atmospheric nano-particles. *Nature Communications*, 7, 11594. Copyright - Copyright Nature Publishing Group May 2016; Last updated - 2016-05-21.

[Makkonen et al., 2012] Makkonen, R., Asmi, A., Kerminen, V.-M., Boy, M., Arneth, A., Hari, P., & Kulmala, M. (2012). Air pollution control and decreasing new particle formation lead to strong climate warming. *Atmospheric chemistry and physics*, 12(3), 1515–1524.

[Matheson et al., 2005] Matheson, M. A., Coakley, J. A., & Tahnk, W. R. (2005). Aerosol and cloud property relationships for summertime stratiform clouds in the northeastern atlantic from advanced very high resolution radiometer observations. *Journal of Geophysical Research: Atmospheres*, 110(D24).

[Mirme & Mirme, 2013] Mirme, S. & Mirme, A. (2013). The mathematical principles and design of the nais – a spectrometer for the measurement of cluster ion and nanometer aerosol size distributions. *Atmospheric Measurement Techniques*, 6(4), 1061–1071.

[Ng et al., 2011] Ng, N. L., Herndon, S. C., Trimborn, A., Canagaratna, M. R., Croteau, P., Onasch, T. B., Sueper, D., Worsnop, D. R., Zhang, Q., Sun, Y., et al. (2011). An aerosol chemical speciation monitor (acsm) for routine monitoring of the composition and mass concentrations of ambient aerosol. *Aerosol Science and Technology*, 45(7), 780–794.

[O'Dowd & Wagner, 2007] O'Dowd, C. D. & Wagner, P. E. (2007). *Nucleation and Atmospheric Aerosols: 17th International Conference, Galway, Ireland, 2007*. Springer Science & Business Media.

[Pandis et al., 1995] Pandis, S. N., Wexler, A. S., & Seinfeld, J. H. (1995). Dynamics of tropospheric aerosols. *The Journal of Physical Chemistry*, 99(24), 9646–9659.

[Pirjola et al., 1999] Pirjola, L., Kulmala, M., Wilck, M., Bischoff, A., Stratmann, F., & Otto, E. (1999). Formation of sulphuric acid aerosols and cloud condensation

nuclei: An expression for significant nucleation and model comprarison. *Journal of Aerosol Science*, 30(8), 1079–1094.

[Pruppacher, 1998] Pruppacher, H. (1998). Hr pruppacher, jd klett, and pk wang, microphysics of clouds and precipitation, aerosol sci. technol. 28, 381 (1998). *Aerosol Sci. Technol.*, 28, 381.

[Pöschl, 2005] Pöschl, U. (2005). Atmospheric aerosols: Composition, transformation, climate and health effects. *Angewandte Chemie International Edition*, 44(46), 7520–7540.

[Ramanathan & Feng, 2009] Ramanathan, V. & Feng, Y. (2009). Air pollution, greenhouse gases and climate change: Global and regional perspectives. *Atmospheric Environment*, 43(1), 37 – 50. Atmospheric Environment - Fifty Years of Endeavour.

[Rönkkö et al., 2017] Rönkkö, T., Kuuluvainen, H., Karjalainen, P., Keskinen, J., Hillamo, R., Niemi, J. V., Pirjola, L., Timonen, H. J., Saarikoski, S., Saukko, E., Järvinen, A., Silvennoinen, H., Rostedt, A., Olin, M., Yli-Ojanperä, J., Nousiainen, P., Kousa, A., & Dal Maso, M. (2017). Traffic is a major source of atmospheric nanocluster aerosol. *Proceedings of the National Academy of Sciences*, 114(29), 7549–7554.

[Rosenfeld et al., 2014] Rosenfeld, D., Sherwood, S., Wood, R., & Donner, L. (2014). Climate effects of aerosol-cloud interactions. *Science*, 343(6169), 379–380.

[Seinfeld & Pandis, 2006] Seinfeld, J. H. & Pandis, S. N. (2006). *Atmospheric chemistry and physics: from air pollution to climate change*. John Wiley & Sons.

[Tie et al., 2009] Tie, X., Wu, D., & Brasseur, G. (2009). Lung cancer mortality and exposure to atmospheric aerosol particles in guangzhou, china. *Atmospheric Environment*, 43(14), 2375 – 2377.

[Vanhanen et al., 2011] Vanhanen, J., Mikkilä, J., Lehtipalo, K., Sipilä, M., Manninen, H. E., Siivola, E., Petäjä, T., & Kulmala, M. (2011). Particle size magnifier for nano-cn detection. *Aerosol Science and Technology*, 45(4), 533–542.

[Vehkamäki, 2006] Vehkamäki, H. (2006). *Classical nucleation theory in multicomponent systems*. Berlin: Springer.

[Wang & Flagan, 1990] Wang, S. C. & Flagan, R. C. (1990). Scanning electrical mobility spectrometer. *Aerosol Science and Technology*, 13(2), 230–240.

[Winkler et al., 2008] Winkler, P. M., Steiner, G., Vrtala, A., Vehkamäki, H., Noppel, M., Lehtinen, K. E., Reischl, G. P., Wagner, P. E., & Kulmala, M. (2008). Heterogeneous nucleation experiments bridging the scale from molecular ion clusters to nanoparticles. *Science*, 319(5868), 1374–1377.

[Wu et al., 2008] Wu, Z., Hu, M., Lin, P., Liu, S., Wehner, B., & Wiedensohler, A. (2008). Particle number size distribution in the urban atmosphere of beijing, china. *Atmospheric Environment*, 42(34), 7967–7980.

[Xiao et al., 2015] Xiao, S., Wang, M., Yao, L., Kulmala, M., Zhou, B., Yang, X., Chen, J., Wang, D., Fu, Q., Worsnop, D., et al. (2015). Strong atmospheric new particle formation in winter in urban shanghai, china. *Atmospheric Chemistry and Physics*, 15(4), 1769–1781.

[Yao et al., 2018] Yao, L., Garmash, O., Bianchi, F., Zheng, J., Yan, C., Kontkanen, J., Junninen, H., Mazon, S. B., Ehn, M., Paasonen, P., et al. (2018). Atmospheric new particle formation from sulfuric acid and amines in a chinese megacity. *Science*, 361(6399), 278–281.

[Zhang et al., 2012] Zhang, R., Khalizov, A., Wang, L., Hu, M., & Xu, W. (2012). Nucleation and growth of nanoparticles in the atmosphere. *Chemical Reviews*, 112(3), 1957–2011. PMID: 22044487.